

FINAL REPORT

Environmental Impact of DNAN and NTO on Plants

Timothy Cary
ERDC-CRREL

Neil Bruce
Elizabeth Rylott
University of York

May 2025

SERDP FINAL REPORT

Project: ER-2723

TABLE OF CONTENTS

	Page
ABSTRACT	VI
EXECUTIVE SUMMARY	ES-1
1.0 BACKGROUND	1
2.0 MATERIALS AND METHODS.....	3
2.1 AGAR PLATE EXPERIMENTS	3
2.2 T-DNA INSERTION PLANT LINE EXPERIMENTS	3
2.3 GENE VECTORS.....	3
2.4 RECOMBINANT PROTEIN PRODUCTION.....	3
2.5 DNAN PHYTOTOXICITY STUDIES	4
2.6 HPLC ANALYSIS.....	4
2.7 METHANOL EXTRACTS	4
2.8 MDHAR6 ACTIVITY ASSAYS	4
2.9 SOIL STUDIES	5
2.10 HYDROPONIC EXPERIMENTS.....	5
2.11 TRANSCRIPTOMICS ANALYSIS.....	5
2.12 OPR ACTIVITY ASSAYS.....	5
2.13 GLUTATHIONE TRANSFERASE ACTIVITY	6
2.14 STATISTICAL ANALYSIS	6
3.0 RESULTS AND DISCUSSION	7
3.1 TASK 4. – ESTABLISHING THE MECHANISM OF DNAN AND NTO TOXICITY	7
3.1.1 Task 4.1 Screening mutant Arabidopsis populations on media with DNAN and NTO	9
3.1.2 Task 4.2 Characterizing allelic mutant, overexpression and knock-down Arabidopsis lines.....	11
3.2 TASK 5. DETERMINING DEGRADATION INTERMEDIATES	13
3.2.1 Task 5.1 Measuring DNAN, NTO and transformation products using liquid cultures	13
3.2.2 Task 5.2 Determining in-planta location of DNAN and NTO at the organ level.....	16
3.3 TASK 6. BIOCHEMICAL PATHWAY CHARACTERIZATION.....	17
3.3.1 Task 6.1 Measuring gene expression in response to DNAN	17
3.3.2 Task 6.2 Plant lines with modified target gene expression levels.....	35
4.0 CONCLUSIONS AND IMPLICATIONS FOR FUTURE RESEARCH/IMPLEMENTATION.....	38

TABLE OF CONTENTS (Continued)

	Page
4.1 OBJECTIVE 3. ELUCIDATED MECHANISMS OF DNAN AND NTO TOXICITY IN PLANTS	38
4.2 OBJECTIVE 4. IDENTIFICATION OF THE <i>IN PLANTA</i> DETOXIFICATION INTERMEDIATES OF DNAN AND NTO IN ARABIDOPSIS.....	39
4.3 OBJECTIVE 5. RESOLVED BIOCHEMICAL PATHWAYS FOR THE DETOXIFICATION OF DNAN AND NTO IN PLANTS	39
4.4 CONCLUSION.....	40
5.0 LITERATURE CITED	41

LIST OF FIGURES

	Page
Figure ES-1. Summary of the Biotransformation Routes of (a) DNAN and (b) NTO. Figure is Based on Olivares et al., 2016 and Le Campion et al., 1999.	ES-2
Figure 2. The Effect of Different Concentrations of (a) DNAN and (b) TNT on Growth of Arabidopsis Seeds ($n = 48 \pm \text{SD}$).	7
Figure 3. The Effect of DNAN on Arabidopsis Plant (a) Shoots and (b) Roots.	8
Figure 4. The Effect of Different Concentrations of NTO on Root Growth of Arabidopsis Seeds.....	8
Figure 5. (a) Arabidopsis Seedlings after Fourteen Days of Growth on 1/2 MS Media Containing 50 μM of DNAN. (b) Plant Phenotypes Proscribed a Particular Fitness Score.....	9
Figure 6. Root Length of Mutant Arabidopsis Lines Grown on Solid Agar with Either 0 or 50 μM DNAN.....	10
Figure 7. Arabidopsis root lengths of mdhar6 mutants and WT seedling grown on solid agar with and without 50 μM DNAN.....	12
Figure 8. Six-week-old mdhar6 Mutant and WT Plants Grown on 100 mg/kg Soil.	12
Figure 9. (a) SDS-PAGE Gel of Recombinantly Expressed, Purified MDHAR6 Protein. (b) Activity of MDHAR6 Activity on TNT and DNAN Substrate ($n = 3 \pm \text{SD}$). (c) Amount of DNAN and TNT Remaining in the Reaction after 24 Hours in the Presence of Enzymatic NADH-recycling System.	13
Figure 10. Phytotoxicity of DNAN and TNT on Arabidopsis.....	14
Figure 11. A) DNAN and Nitro-reduced Derivates within Arabidopsis Tissue 4 and 7 Days Post Dosing. (B) Chromatogram of Tissue Extracts from Arabidopsis Dosed with 250 μM of DNAN Compared to the Undosed Control.	15
Figure 12. Effect of Different Concentrations of DNAN and Its Amino Derivatives on Arabidopsis (a) Seedling Root Length ($n > 24 \pm \text{SD}$) and (b) Seedling Biomass ($n = 3 \pm \text{SD}$).	15
Figure 13. Fresh Weight of Two-week-old Arabidopsis Plants Grown in Liquid Culture, Seven-days Post Dosing.	16
Figure 14. Location of Xenobiotic Compounds in Arabidopsis Plants.	17
Figure 15. Electrophoresis Run Summary of the 0 μM and 60 μM DNAN Conditions.	18
Figure 16. Differential Expression of Arabidopsis Transcripts in the Presence of 480 μM DNAN.	19
Figure 17. Gene Ontology (GO) of Genes Upregulated in Response to DNAN.....	20
Figure 18. Abundance of Glutathione Transferase (GST) from the TAU Subfamily in Arabidopsis Plants Exposed for Six Hours to DNAN.	21
Figure 19. SDS-PAGE Analysis of the Recombinantly Expressed and Purified GSTs.	22
Figure 20. Activity of Recombinantly Produced GSTs on Substrate.	23
Figure 21. Abundance of Glycosyltransferase (UGT) Transcripts in Arabidopsis Plants across a Range of DNAN Concentrations.....	24

LIST OF FIGURES

	Page
Figure 22. Transformation of TNT by oxophytodienoate reductases (OPR). Sourced from (Beynon et al., 2009).	25
Figure 23. Counts per million (CPM) of Oxophytodienoate Reductases (OPR) Gene Responses to Varying Concentrations of DNAN.	26
Figure 24. Recombinant Protein Production and Activity of the OPRs and ONR Control.....	26
Figure 25. Growth of 35S-OPR Overexpressor Plant Lines in TNT or DNAN Dosed Media.	27
Figure 26. Abundance of Multidrug Resistance (MDR) Transcripts, from Subfamily C of ABC Transporters, Across a Range of DNAN Concentrations.	28
Figure 27. Counts per Million (CPM) of Gamma-glutamyl Transpeptidase (ggt3; AT4G29210), o-malonyltransferase (AT5G39050) and Sulfotransferase (AT2G03760) Gene Responses to Varying Concentrations of DNAN.	28
Figure 28. Root Length of Wildtype and <i>mrp2</i> Mutant Arabidopsis Lines Grown on Solid Agar with Either 0 or 20 μ M DNAN.....	29
Figure 29. Differential Expression of <i>A. thaliana</i> Transcripts in the Presence of 300 and 600 μ M NTO.....	30
Figure 30. Abundance of Plant Defensin (PDF) Transcripts in Arabidopsis Plants across a Range of NTO Concentrations.	31
Figure 31. Abundance of Glycosyltransferase Transcripts in Arabidopsis Plants Across a Range of NTO Concentrations.	32
Figure 32. Abundance of Cytochrome P450 (CYP) Transcripts in Arabidopsis Plants Across a Range of NTO Concentrations.	33
Figure 33. Western Blot of the Recombinantly Produced <i>A. thaliana</i> GSTs.	34
Figure 34. Concentrations of NTO Remaining after Incubating with GST Enzymes and Glutathione.	35
Figure 35. Root Lengths of Arabidopsis Plant Lines Grown on Different Concentrations of NTO.	36
Figure 36. Growth of Wildtype and <i>FoxI</i> Mutant Lines Grown in the Presence DNAN and TNT.....	37

LIST OF TABLES

	Page
Table 1. Fitness Scores for Mutant Arabidopsis Libraries.....	10
Table 2. NASC ID of Mutant Lines that Grew Significantly Better than Wild Type in the Presence of DNAN.	11
Table 3. Number of Genes Differentially Expressed (P>0.001) after 6 Hours of Exposure to DNAN Compared to Control Conditions.	18
Table 4. Specific activities of the GSTs in the presence of glutathione and CDNB substrates. Specific activity units are nmol substrate per minute per mg of enzyme. N.D. – No data.	34

ABSTRACT

INTRODUCTION AND OBJECTIVES

Explosives are widespread chemicals of concern at DoD training ranges. Current munition compositions such as Composition B mainly comprise 2,4,6-trinitrotoluene (TNT) and 1,3,5-trinitrohexahydro- triazine (RDX); both compounds are toxic and a threat to environmental ecosystems. New composition mixtures containing 2,4-dinitroanisoole (DNAN) and 3-nitro-1,2,4-triazol-5-one (NTO) are currently being phased in as replacements for Composition B to improve the safety of munitions. In this project we will integrate the knowledge gained from the proposed plant and soil studies to develop a mechanistic understanding and predictive capability of the fate and impact of these compounds in the environment. The findings from this project will facilitate the development of strategies to ensure the impact on DoD sites is minimal thus mitigating costs associated with the deployment of future remedial and control technologies. The proposed work responds directly to the specific research objectives in Statement of Need (SON) number ERSON- 17-03 to determine effects of insensitive munitions compounds on vegetation in terms of toxicity and uptake.

TECHNICAL APPROACH

In Task 4, we first established the toxicity of DNAN and NTO on Arabidopsis plants and then carried out a high-throughput screen of Arabidopsis mutants. T-DNA insertional mutants were obtained from the Nottingham Arabidopsis Stock Centre (NASC). Mutants were scored for ability to grow on DNAN media and genes identified that may be facilitating plant growth.

Previous studies that were funded by SERDP ER-1498 identified that monodehydroascorbate reductase 6 (MDHAR6) was a key driver of TNT toxicity in Arabidopsis plants. Due to the chemical similarity between TNT and DNAN, we tested whether MDHAR6-mutant plants have increased ability to degrade DNAN.

In Task 5, we sought to characterize the breakdown and transformation products of DNAN. Using shake flasks and high performance liquid chromatography (HPLC) analysis, we monitored the levels of DNAN and NTO over time in media. We then set up hydroponic experiments in order to determine the concentrations of DNAN and transformation products in plant biomass. We also determined the toxicity of DNAN transformation products on plant germination and growth.

In Task 6, we carried out transcriptomic analysis of Arabidopsis plants grown on DNAN- and NTO-containing media. This identified genes differentially expressed in response to DNAN and NTO. Any enzymes that were differentially expressed and associated with xenobiotic biodegradation pathways were taken for recombinant expression and purification. The enzymes were then biochemically characterized to inform on their role in DNAN and NTO biodegradation in plants.

RESULTS

Of the Arabidopsis mutants with increased fitness scores over wildtype in the DNAN toxicity studies, none of the genes were associated with known xenobiotic detoxification pathways. This is likely due to redundancy in the detoxification pathways in the plants. In addition, knockout of MDHAR6 in Arabidopsis plants also enhanced plant fitness, confirming our hypothesis that MDHAR6 plays a role in DNAN toxicity.

Uptake of DNAN into Arabidopsis plants from media was slower than TNT. 2ANAN (2-amino-4-nitroanisole; 2-methoxy-5-nitroaniline) was identified to be a major amino derivative produced. Interestingly, DNAN significantly impaired root growth in seedlings and plant growth, whereas 2ANAN had little effect on seedling root length but significantly impaired plant growth. This may be due to the different lifecycle stages of the plants to measure root length (seedling) and plant biomass (plants). Whereas DNAN was detectable in both the roots and shoots of plants, only the reduction products of TNT were detectable in the roots. This suggests plants can more rapidly breakdown TNT than DNAN.

Transcriptomic analysis was carried in order to try and identify detoxification pathways of DNAN and NTO in plants. In the presence of 480 μ M DNAN, 2330 transcripts were upregulated, many of which were associated with nitroreduction, conjugation and transport. In the presence of 600 μ M NTO.

The TAU subfamily of glutathione S-transferases (GSTs) were one such family of conjugating enzymes upregulated. After excluding low-expressing GSTs, GST TAU 24 and 25 were most upregulated. Though less strongly upregulated, GST TAU 19 had the greatest transcript abundance. GST TAU 1, 2, 4, 7, 9, 19, 22, 24 and 25 were recombinantly expressed and purified. Though each at least had a minimal amount of activity on CDNB substrate, there was no evidence of conjugating activity on DNAN. Uridine diphosphate-glycosyltransferases (UGTs) were also upregulated in the transcriptome, including UGT74E2 which was the third most upregulated gene in the entire transcriptome.

Members of the oxophytodienoate reductases (OPR) family were also upregulated in the presence of DNAN. OPR 1, 2 and 4/5 were each recombinantly expressed and purified. The OPRs were able to nitroreduction of DNAN, though less so than TNT. Biomass of two-week old OPR-overexpressor Arabidopsis plants dosed with either TNT or DNAN were unaffected. However, subtle differences were observed in the media. OPR1-overexpressor lines had a significant reduction in DNAN and OPR2 overexpressor lines had a small significant increase in 2ANAN.

Other notable genes upregulated include five multidrug resistance-associated proteins (MRPs) that may have a role in transport of glutathione (GSH) conjugates. However, the most upregulated MRP is part of a different subfamily that do not transport glutathione conjugates. Though upregulated, the root lengths of *mrp2* knock-out plant lines were unaffected. Finally, an *o*-malonyltransferase and sulfotransferase were also upregulated. These enzymes warrant further investigation in their involvement of toxicity and detoxification of DNAN.

BENEFITS

Investigations into the impact of DNAN and NTO on plants will provide a clearer understanding of the fate of these compounds in field settings. The availability of bench mark data regarding the transport and fate of the energetic materials will support predictions and modeling. These models will enable the DoD to use best management practices in identifying training ranges with ecosystems that are particularly sensitive to DNAN and NTO, and allow the identification of others that present an acceptable risk. The results obtained will provide potential cost savings, since such knowledge will mitigate contamination and alleviate the need for future clean-up operations.

EXECUTIVE SUMMARY

INTRODUCTION

Explosives are widespread contaminants at DoD training ranges such that both land and groundwater are severely contaminated. Current munition compositions such as Composition B mainly comprise 2,4,6-trinitrotoluene (TNT) and 1,3,5-trinitrohexahydro- triazine (RDX); both compounds are toxic and a threat to environmental ecosystems. Whilst TNT and its transformation products bind strongly to clay and organic matter in soils, RDX is far more mobile posing significant off base groundwater contamination risks. New composition mixtures containing 2,4-dinitroanisole (DNAN) and 3-nitro-1,2,4-triazol-5-one (NTO) are currently being phased in as replacements for Composition B to improve the safety of munitions. Relatively low aqueous solubility of DNAN means that, like TNT, it binds to organic matter in soil. However, each successive reduction of the nitro groups to amines reduces the hydrophobicity and increases migration potential through the soil. NTO and reported transformation products are far more water soluble and so also highly mobile in soils. Therefore, the new composition mixtures pose significant risks of land and groundwater contamination.

Little is known about the effects of DNAN and NTO on plants, except soil studies that showed DNAN and IMX-101 (mixture of DNAN, NTO and 1-nitroguanidine) were toxic to grasses (Dodard et al., 2013; Richard and Weidhaas, 2014). However, microbial degradation pathways of DNAN have been identified and characterized from mixed consortia and pure cultures under aerobic and anaerobic conditions (Fida et al., 2014; Hawari et al., 2015; Liang et al., 2013; Perreault et al., 2012; Platten et al., 2010) as well as an endophytic bacterium isolated from willow (Schroer et al., 2015). The currently understood biodegradation pathway involves reduction of nitro groups to aromatic amines via a series of nitroso-intermediates (Figure ES-1). Reduction of the *ortho* nitro group is preferred in the reactions. Coupling can occur between nitroso-intermediates and aromatic amines to form azo dimers. Functional groups of azo dimers can then undergo further transformations such as demethylation, demethoxylation and dehydroxylation (Liang et al., 2013; Olivares et al., 2013, 2016a; Perreault et al., 2012). Longer term fate of these azo dimers are not known.

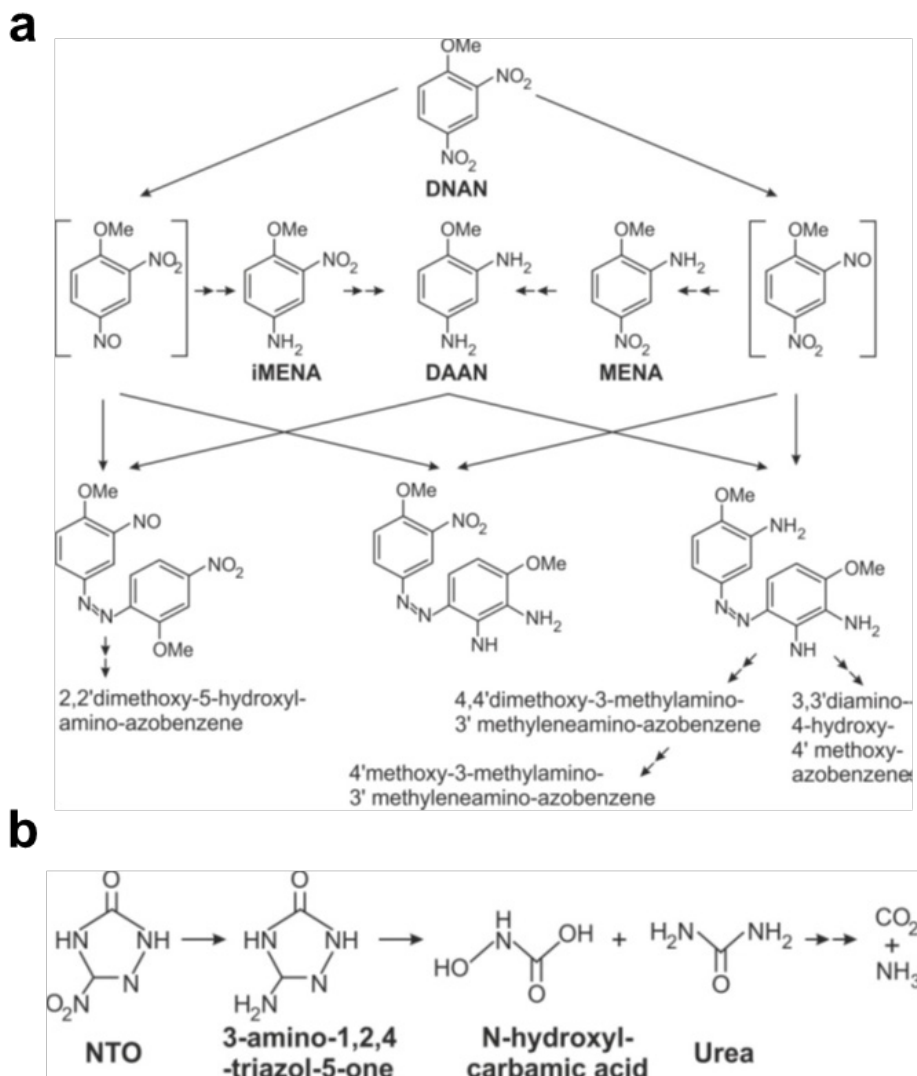


Figure ES-1. Summary of the Biotransformation Routes of (a) DNAN and (b) NTO. Figure is Based on Olivares et al., 2016 and Le Campion et al., 1999.

Less is known about the biodegradation of NTO. Microbial transformation studies in *Bacillus licheniformis* showed that NTO is transformed to 3-amino-1,2,4-triazol-5-one (ATO). Ring cleavage then occurs to generate N-hydroxyl-carbamic acid and urea (Le Campion et al., 1999) which can then be mineralized.

Toxicity studies on plants are limited and generally have been conducted using insensitive munition mixtures such as IMX-101. DNAN has been shown to inhibit seed germination and plant growth (Taylor et al., 2015) and is toxic to bacteria and earthworms (Dodard et al., 2013). Richard and Weidhass studied uptake of DNAN and NTO in the IMX-101 formulation but interestingly only found uptake of DNAN in the plant roots (Richard and Weidhaas, 2014). However, the compounds were not in pure form and so the results may not be relevant to our study. Inhibitory concentrations of NTO in aquatic ecosystems have been determined on *Ceriodaphnia dubia* and *Selenastrum capricornutum* freshwater organisms (Haley et al., 2009).

Toxicity thresholds are critical to understand the ecological impacts of accidental release, better manage landscapes and generate new plant DNAN- and NTO-resistant germplasms. Therefore, toxicity thresholds of DNAN and NTO requires further research.

OBJECTIVES

In this project, the primary objective will be to rigorously establish the fate and effects of DNAN and NTO on plants and the environment. This includes understanding the physicochemical parameters of the compounds in the soil and assessing the toxicity of the compounds on plant species native to U.S. military training ranges. Further to this, we will elucidate mechanisms of NTO and DNAN toxicity in plants, identify *in planta* transformation intermediates of the compounds in Arabidopsis and, finally, resolve the biochemical pathways for the detoxification of these compounds in plants.

The findings from this project will facilitate the development of strategies to ensure the impact on DoD sites is minimal thus mitigating costs associated with the deployment of future remedial and control technologies. The proposed work responds directly to the specific research objectives in Statement of Need (SON) number ERSON- 17-03 to determine effects of insensitive munitions compounds on vegetation in terms of toxicity and uptake.

TECHNICAL APPROACH

In Task 4, we first sought to establish the toxicity of DNAN on wildtype Arabidopsis plants by growing seedlings on ½ MS agar plates containing a range of DNAN concentrations. A toxicity curve was then generated for DNAN and TNT as a comparison. After establishing the toxicity of DNAN, a high-throughput screen of Arabidopsis mutants was set up in order to try and identify genes that contribute to DNAN toxicity in the plant. T-DNA insertional mutants were obtained from the Nottingham Arabidopsis Stock Centre (NASC). Seeds were then germinated and grown up on ½ MS agar plates, in a 6-well plate format, dosed with 50 µM DNAN. After 14 days, seedlings were given a fitness score for ability to grow on 50 µM DNAN. Mutants with the highest fitness score were then grown on ½ MS agar plates and root lengths measured. Those with root lengths significantly greater than wildtype were identified and checked if the mutant gene was known to be linked to xenobiotic degradation pathways.

Previous studies that were funded by SERDP ER-1498 identified that monodehydroascorbate reductase 6 (MDHAR6) was a key driver of TNT toxicity in Arabidopsis plants. TNT and DNAN have high chemical similarity, thus we hypothesized that MDHAR6 may also play role in DNAN toxicity in plants. Wildtype and MDHAR6-mutant Arabidopsis plants were grown on media containing 50 µM DNAN and root lengths measured. Further to this, wildtype and MDHAR6-mutant plants were also grown on soil with DNAN at concentrations of either 0 or 100 mg/kg. MDHAR6 was recombinantly expressed, purified and assayed *in vitro* with DNAN substrate to confirm activity.

In Task 5, we sought to characterize the breakdown and transformation products of DNAN. First, liquid cultures were set up to compare phytotoxicity of DNAN and TNT across a range of concentrations. Fresh weights of plants were measured. Uptake and breakdown of the compounds were monitored using HPLC by determining the concentration of each compound remaining in the media.

Next, tissue of seedlings in shake flasks at day 4 and 7 were methanol extracted and analyzed for the presence of amino derivatives. Toxicity of the amino derivatives on Arabidopsis plants was then determined by measuring root length from seedlings grown on ½ MS agar plates and measuring plant biomass from seedlings grown up in shake flasks. Finally, we set up hydroponic experiments in order to determine the concentrations of DNAN and transformation products in plant biomass. Plants were also grown in media containing TNT as a comparison. Plants were germinated and transferred to the hydroponic system with either 125 µM or 250 µM compound. Roots and shoots were separately methanol extracted and analyzed by HPLC.

In Task 6, we carried out transcriptomic analysis of Arabidopsis plants grown on DNAN- and NTO-containing media. Arabidopsis plants were grown up in shake flasks containing from 0-480 µM DNAN and the RNA extracted from plant tissue. RNA sample quality was assessed by TapeStation (Agilent) gel capillary electrophoresis. Messenger RNA (mRNA) was enriched for by poly(A) selection. Sequencing of mRNA was performed using the Illumina HiSeq 3000 platform. Gene ontology (GO) analysis was then performed on the differentially expressed RNA transcripts in order to identify genes associated with xenobiotic detoxification pathways. Interesting enzyme families were taken for recombinant expression and purification. The enzymes were then biochemically characterized to inform on their role in toxicity and biodegradation of DNAN and NTO in plants.

RESULTS AND DISCUSSION

Task 4: Establishing the mechanism of DNAN and NTO toxicity

Initial toxicity studies of DNAN and TNT on wildtype Arabidopsis plants established that both compounds significantly reduced root length and plant biomass. Toxicity was more acute at higher concentrations of TNT. Greater than 75% plant biomass was lost when grown on 50 µM DNAN, compared to approximately 98% plant biomass lost in the presence of 50 µM TNT. In the presence of 600 µM NTO, root lengths were greater than 30% smaller, seemingly less phytotoxic than TNT and DNAN. Next, T-DNA insertional Arabidopsis mutants obtained from NASC were grown up on 50 µM DNAN and given a fitness score based on the seedlings ability to grow on the media. Highest fitness lines (155) were then grown up on 50 µM DNAN and root lengths measured. Sixteen mutants had significantly greater root length than wildtype. However, none of these had mutations in genes known to be associated with xenobiotic degradation (Ramel et al., 2012). This report later details that some genes represented in this screen can degrade DNAN, such as the OPRs (Task 6). No observable change in root length was observed for these plant mutants, indicating redundancy in xenobiotic degradation pathways.

Our previous studies (funded by SERDP ER-1498) identified that MDHAR6 was strongly associated with toxicity in plants exposed to TNT. *mdhar6* mutants grew significantly better than wildtype plants exposed to TNT (Johnston et al., 2015). DNAN and TNT share significant chemical similarity so *mdhar6* mutant and wildtype plants were exposed to DNAN. Mutants had greater root lengths and plant biomass. Soil studies replicated this data confirming that MDHAR6 has a role in DNAN toxicity in plants. Recombinantly produced MDHAR6 was also confirmed to have activity on DNAN, albeit minimal compared to TNT. In the presence of an NADH-recycling system, DNAN was not depleted by MDHAR6, also suggesting that, like TNT, toxicity in the plant is due to a futile cycle being established.

Task 5: Determining degradation intermediates

Liquid cultures were set up in order to determine relative phytotoxicities of DNAN and TNT. Interestingly, whilst at 250 μM , the greatest decrease in biomass was observed for TNT, at 50 μM , DNAN caused the greater decrease in biomass. HPLC analysis of the media identified that TNT was rapidly depleted whereas DNAN persisted for much longer. This might explain the more chronic toxicity observed at 50 μM DNAN. Methanol extracted tissue from seedlings dosed with 250 μM DNAN indicated that plants can reduce DNAN to 2ANAN (and a small amount of 4-amino-2-nitroanisole, 4ANAN). This conversion is likely a key step in detoxification of DNAN.

Nitro-reduced products have been reported to be less toxic in zebrafish and microbes (Liang et al., 2013; Olivares et al., 2016b), but little is known in regard to plants. We sought to establish the toxicity of 2ANAN, 4ANAN and 2,4-diaminoanisole (DAAN) to Arabidopsis plants. Interestingly, phytotoxicity experiments showed that DNAN significantly reduced root length and plant biomass, whereas 2ANAN only significantly affected plant biomass. This is likely due to the different developmental stages of plants used to measure root length and biomass. 4ANAN and DAAN had little effect at concentrations of less than 100 μM .

Locations of the xenobiotics in plants was investigated by a hydroponic system exposing plants to DNAN or TNT. Analysis of media indicated that DNAN was less readily taken up by the plants than TNT. Methanol extracted tissue indicated that only nitro-reduced products 2-amino-4,6-dinitrotoluene (2ADNT) and 4-amino-2,6-dinitrotoluene (4ADNT) of TNT were present in the roots. However, DNAN and 2ANAN were detected in both roots and shoots of plants. These data suggest that TNT is more readily transformed by plants.

As for TNT and DNAN, liquid cultures were set up for NTO containing up to 1000 μM xenobiotic. Cultures had to be buffered with 50 mM HEPES to prevent acidification by NTO. Interestingly, very little difference in biomass was observed after seven days. This seems at odds to the root lengths toxicity data, but could be due to the different developmental stages of the plants tested (as suggested for 2ANAN).

Task 6: Biochemical pathway characterization

We next sought to identify and characterize biochemical pathways involved in detoxification of DNAN. Seedlings were grown up in shake flasks dosed with concentrations ranging 0-480 μM DNAN. RNA was extracted from the plants and sequenced. Sequence analysis identified 2330 transcripts upregulated in 480 μM DNAN. GO analysis indicated that some of the most upregulated transcripts were associated with nitroreduction, conjugation and transport. This was in agreement with previous studies on other xenobiotic compounds (Ramel et al., 2012). Of particular interest, a number of enzyme families were upregulated, including GSTs, UGTs and OPRs.

We previously demonstrated that GSTs can conjugate TNT to glutathione and thus prevent MDHAR6-driven phytotoxicity of TNT (Gunning et al., 2014; Johnston et al., 2015). Moreover, DNAN-glutathione conjugates have been described in Arabidopsis (Schroer et al., 2017). Therefore, it was not surprising that 17 GSTs were upregulated in the presence of DNAN. GST TAU 24 and 25 were most upregulated; these enzymes are known to conjugate TNT to glutathione (Gunning et al., 2014). Notably GST TAU 19 had by far the greatest abundance of transcripts.

Nine of these GSTs were recombinantly expressed and purified from *E. coli*. Assays containing 1-chloro-2,4-dinitrobenzene (CDNB) and reduced GSH confirmed activity of each of these enzymes. Under similar conditions that conjugation of TNT was observed, the GSTs only had minimal activity on DNAN with no significant depletion of the compound observed.

UGTs are known to be upregulated in response to TNT, however conjugation to an activate nucleotide sugar group can only occur to the hydroxylamino dinitrotoulene (HADNT) or amino dinitrotoulene (ADNT) derivatives (Gandia-Herrero et al., 2008; Ross et al., 2001). In the presence of DNAN, 21 of the 107 *Arabidopsis* UGTs considered in the transcriptomic analysis were upregulated. Six of these are known to conjugate HADNT and ADNT. Future investigation into these enzymes is warranted to understand their possible role in conjugation of DNAN derivatives.

OPRs can catalyze the activation of TNT for conjugation to glucose. Through oxidation of NAD(P)H, OPRs concurrently reduce nitro groups to ADNT and HADNT products (Beynon et al., 2009). The *Arabidopsis* OPR family consists of six genes, whereby OPR4 and OPR5 are duplications of one another (Beynon et al., 2009). OPR1, OPR2 and OPR4/5 were upregulated in the presence of DNAN. OPR1, OPR2 and OPR4/5 were each recombinantly expressed and purified from *E. coli*. OPR1, OPR2 and OPR4/5 had activity on DNAN substrate, albeit minimal compared to TNT substrate. OPR1 and OPR2 are only expressed in plant roots whereas OPR4/5 is expressed in plant shoots (Beynon et al., 2009). This suggests OPR1 and OPR2 could contribute to accumulation of 2ANAN in the roots whereas OPR4/5 contributes to accumulation in the shoots. Next, 35S-OPR overexpressor *Arabidopsis* plant lines were generated. 35S-OPR overexpressor lines were grown in media dosed with DNAN or TNT. After seven days, there was no significant difference in plant biomass from wildtype. However, analysis of the growth media hinted at some subtle differences. 35S-OPR1 lines contained significantly less DNAN in the media after seven days. Conversely, a significant increase in 2ANAN was observed in 35S-OPR2 line media. These data suggest that OPR1 and OPR2 may contribute to the breakdown of DNAN in plants.

Our transcriptomic analysis also identified a few other notable genes upregulated, including five MRPs. These proteins have been identified to have a role in transport of glutathione (GSH) conjugates (Klein et al., 2006; Lu et al., 1997). However, the most upregulated AtMRP3 is part of a different subfamily which does not transport glutathione conjugates. Glutathione conjugates may undergo further processing inside the vacuole (Coleman et al., 1997). Gamma-glutamyl transpeptidases (GGTs) catalyze cleavage of Glu-Cys peptide bonds, of which *Arabidopsis* expresses four GGTs. Only GGT3 is localized to vacuoles but has been demonstrated to have activity on other conjugated xenobiotics (Ohkama-Ohtsu et al., 2007). However, this enzyme was not upregulated in the presence of DNAN in our analysis. Finally, an o-malonyltransferase and sulfotransferase were also upregulated. Indeed, malonylation of xenobiotics has been reported to increase their accumulation inside the cell (Taguchi et al., 2010). These enzymes warrant further investigation in their involvement of toxicity and detoxification of DNAN.

Transcriptomic analysis was also carried out on plants grown in the presence of NTO. Concentrations of 0-600 μ M NTO were used, RNA extracted and sequenced. Significantly fewer transcripts were differentially expressed in our analysis, indicative of the less phytotoxic effects of NTO on plants. Transcripts were upregulated in the presence of 600 μ M NTO. A number of gene families were upregulated including MATE efflux transporters known to export xenobiotics (Gandia-Herrero et al., 2008), plant defensins that are implicated in heavy metal tolerance in metal

hyperaccumulators (Mirouze et al., 2006), cytochrome P450s, SPX-domain containing proteins that are involved in nutrient signalling (Duan et al., 2008; Secco et al., 2012; Wang et al., 2008) and GSTs already outlined.

GSTU5, 16 and 24 were upregulated in response to NTO and so were recombinantly expressed and purified for characterisation. Though GSTU5 and 24 were confirmed to have conjugating activity on CDNB to GSH, HPLC analysis indicated the enzymes could not conjugate NTO to GSH. These data suggest that the enzymes are likely unable to produce NTO-conjugates in plants.

Some of the upregulated proteins in the transcriptomic analysis were further examined by generating homozygous lines of single or multiple alleles. Seeds to this effect were obtained from NASC and included the MATE efflux transporters *ALMT1* and *DTX18*, *Allene oxide cyclase 2 (AOC2)*, *SPX1* and *BBE/FOX1* (downregulated in the presence of NTO). 1/2 MS agar plate root lengths assays were performed, however no difference was observed to wildtype when dosed with 0, 300 or 600 μ M NTO. These data suggest that these genes may not contribute to phytotoxicity of NTO.

IMPLICATIONS FOR FUTURE RESEARCH AND BENEFITS

In this project, we show that DNAN exerts a more chronic toxicity on plants, evidenced by the slower breakdown of DNAN. NTO appears significantly less toxic, though this may depend on the plant development stage. Like TNT, DNAN toxicity is partially driven by MDHAR6. DNAN is reduced in the plant to the less toxic 2ANAN compound, however the rate of conversion is markedly slower than that observed for TNT into its amino derivatives. DNAN also drives upregulation of a number of enzymes involved in xenobiotic degradation, including GSTs, UGTs and OPRs. In particular, we show *in vitro* that recombinant OPRs can reduce DNAN and may also increase breakdown of DNAN when expressed in plants. NTO drives upregulation of fewer enzymes, though a number of transporters and proteins involved in nutrient signalling were identified. A number of GSTs were also upregulated, however biochemical characterisation these enzymes could not conjugate NTO to GSH.

The combination of significantly slower transformation and conjugation steps of DNAN means that plants are more exposed to the compound much longer than TNT. As a result, MDHAR6 is exposed to DNAN for longer, the key determinant of toxicity in plants. Moreover, lack of conjugation means that DNAN remains more mobile in both root and aerial plant tissue. This poses a greater risk of toxicity to herbivores and the wider food chain. A number of studies have investigated microbial detoxification of DNAN, including identification of a *Nocardioides* species JS1661 strain that was able to breakdown the compound (Fida et al., 2014; Karthikeyan and Spain, 2016; Rylott and Bruce, 2019). However, without long-term effective, low-cost remediation strategies, DNAN poses a significant danger of leaving a poor environmental legacy similar to its predecessor, TNT. Further research is urgently required to address this.

1.0 BACKGROUND

The insensitive munition 2,4-dinitroanisole (DNAN) is being increasingly used as an alternative to 2,4,6-trinitrotoluene (TNT) in explosive preparations as it can be cast and melted more safely. A major component of military munitions worldwide, TNT is classified by the US Environmental Protection Agency (EPA) as a Group C (possible human) carcinogen and toxic to all organisms tested (Rylott et al., 2011b). Furthermore, this compound is often not significantly mineralized in the environment and still present at munition factories and disposal sites dating back to World Wars I and II. The cost of remediating unexploded ordnance discarded military munitions and munition constituents from active training ranges in the US alone is between \$16 billion and \$165 billion (U. S. Government Accountability, 2004). With increasing public concern, it is imperative that replacement compounds do not further contribute to this pollution.

The currently understood route of microbial DNAN transformation involves the reduction of the nitro groups via nitroso- and hydroxyl-intermediates to aromatic amines. Microbial pathways involve coupling between nitroso-intermediates and aromatic amines, leading to the formation of azo dimers and additional transformations. These pathways have been elucidated from a range of mixed consortia and pure cultures in both aerobic and anaerobic conditions (Fida et al., 2014; Hawari et al., 2015; Liang et al., 2013; Perreault et al., 2012; Platten et al., 2010; Schroer et al., 2015). *Nocardioides* sp. can degrade DNAN via the hydrolytic release of methanol to form 2,4-dinitrophenol, a detoxification route that could have evolved by the recruitment of a novel hydrolase to extend the well-characterized 2,4-DNP pathway (Fida et al., 2014).

A fundamental difference between plant and microbial metabolism of xenobiotics is that plants conjugate activated intermediates to a range of molecules such as sugars and glutathione. This decreases the hydrophobicity of the parent compound and results in a conjugated form that is unable to passively cross biological membranes allowing for controlled localization using active transport. Evidence suggests that TNT conjugates are stored in the vacuole and apoplast prior to their incorporation into cellular macromolecular structures such as lignin (Rylott and Bruce, 2019).

There is a considerable chemical similarity between TNT and DNAN (Fig. 1a), with both compounds containing nitro groups at the 2- and 4- positions on methylbenzene and methoxybenzene rings, respectively. With TNT, much of the detoxification steps occur at these nitro groups, with initial transformation catalyzed by oxophytodienoate reductases (OPRs) to form hydroxyl-amino-dinitrotoluenes (HADNT), then amino-dinitrotoluenes (ADNT) (Beynon et al., 2009). In *Arabidopsis*, the OPR family comprises five genes, with OPR4 (At1g17990) and OPR5 (At1g18020) existing as identical duplications of one another. The remaining members, OPR1 (At1g76680), OPR2 (At1g76690) and OPR3 (At2g06050) can reduce TNT, with OPR1 also catalyzing the reductive attack of the aromatic ring, releasing nitrite and producing hydride (H^- -TNT) and dihydride ($2H^-$ -TNT) Meisenheimer TNT adducts (Beynon et al., 2009).

The HADNT and ADNT transformation intermediates of TNT can be conjugated, at either the 2- or 4- isomer positions, to sugars by uridine 5'-diphospho-glucuronosyltransferases (UGTs) (Gandia-Herrero et al., 2008). There is also direct conjugation of TNT, both through the methyl group or by substitution of a nitro group, for sulfur by Tau class glutathione transferases (GSTs) (Gunning et al., 2014; Tzafestas et al., 2017). Tau class GSTs are involved in the detoxification of many other xenobiotics, including herbicides (Kumar and Trivedi, 2018). It might be expected that

DNAN will be subject to similar detoxification routes *in planta*, and glutathione-DNAN conjugates have been described in *Arabidopsis* (Schroer et al., 2017). However, beyond this, nothing more is known about DNAN detoxification pathways in plants.

Monodehydroascorbate reductase 6 (MDHAR6) has been determined as the primary cause of TNT phytotoxicity in *Arabidopsis thaliana* (*Arabidopsis*). Dual-targeted to mitochondria and plastids, MDHAR6 reduces TNT to a nitro-radical, with the concurrent oxidation of NADH. The radical spontaneously autoxidizes back to TNT with the production of superoxides, and this futile cycle continues, depleting NADH, and producing damaging superoxides within critical subcellular environments (Johnston et al., 2015).

While the toxicity of TNT has been well studied and reported in a wide range of plant species, extremely little is known about the effects of DNAN on plants beyond that in soil studies where DNAN and IMX-101 (which contains DNAN, NTO and 1-nitroguanidine) were shown to be toxic to grasses (Dodard et al., 2013; Richard and Weidhaas, 2014). Given the predicted scale of use as a replacement for TNT worldwide, it is urgent that the toxicity and detoxification pathways of DNAN are understood.

2.0 MATERIALS AND METHODS

2.1 AGAR PLATE EXPERIMENTS

Sterile, stratified *Arabidopsis* seeds were imbibed for 2-3 days at 4 °C and then spotted onto 1/2 MS agar (Murashige and Skoog, 1962) in square plates. 1/2 MS agar was dosed with varying concentrations of TNT, DNAN and NTO or DMSO as a control. Plates were placed upright in a growth room at 21 °C in 20 $\mu\text{mol m}^{-2} \text{s}^{-1}$ light with a 16-h photoperiod. Seedling roots were then photographed at days 7, 10 and 14. Seedlings were also weighed on day 14. Root lengths were measured using ImageJ.

2.2 T-DNA INSERTION PLANT LINE EXPERIMENTS

T-DNA insertion mutant seeds were obtained from Nottingham *Arabidopsis* Stock Centre (NASC). This included 6,868 confirmed N27941 homozygous mutants for the DNAN studies and selected differentially expressed gene T-DNA insertions from the Columbia-0 ecotype lines for the NTO studies. Latter insertions were selected based off the transcriptomic analysis. Single or multiple allele homozygous lines for NTO studies were as follows: the MATE efflux transporters ALMT1 (AT1G08430; GK-840D12) and DTX18 (AT3G23550; Salk_062231C), ALLENE OXIDE CYLCASE2 (AT3G25770; SALK_200293C), BBE3/FOX1 (AT1G26380; GK813E08), and SPX1 (AT5G20150; Salk_026927, Salk_143673, and Salk_0394450).

In the DNAN experiments, seeds were germinated under the same conditions used for the agar plate experiments, except that 6-well plates were used containing 50 μM DNAN. Once seeds were spotted onto the 1/2 MS agar, plates were placed flat in a growth room with identical conditions to the agar plate experiments. Seeds were allowed to grow for 14-days and fitness scores assigned to seedlings depending on how well the mutant line could grow on the media.

In the NTO experiments, seeds were again germinated under the same conditions used for the agar plate experiments. 1/2 MS agar in square plates contained either 0, 300, 600 μM NTO as well as 50 mM HEPES to maintain pH 5.7. Plates were placed upright under the same conditions as for the agar plate experiments. Root lengths and seedling biomass were measured in the same way.

2.3 GENE VECTORS

MDHAR6, GSTU1, GSTU2, GSTU4, GSTU5, GSTU7, GSTU9, GSTU16, GSTU19, GSTU22, GSTU24, GSTU25, OPR1, OPR2 and OPR4/5 were all recombinantly produced. GSTU2, GSTU5, GSTU9, GSTU16, GSTU19, GSTU24 and OPR 4/5 were ordered from Twist Bioscience inside a pET100 *E. coli* expression vector.

2.4 RECOMBINANT PROTEIN PRODUCTION

MDHAR6 was expressed in *E. coli* Arctic Express as previously reported (Johnston et al., 2015). GSTU24 and GSTU25 were expressed in *E. coli* BL21(DE3) as previously reported (Gunning et al., 2014). The remaining GSTs were expressed in *E. coli* BL21 pLysS(DE3). OPRs/ONR were expressed in *E. coli* Rosetta-Gami™ 2(DE3). Briefly, transformed colonies were selected from LB agar plates containing the relevant antibiotic selection marker and grown in 50 mL LB cultures

overnight. 10 mL of these cultures was then inoculated into 500 mL autoinduction media (AIM) with antibiotic. Cultures were incubated at 37 °C across the day and transferred to 20 °C overnight, shaking at 180 rpm throughout. Cultures were pelleted at 4000 g for 15 minutes at 4 °C and pellets stored at -20 °C.

Recombinant MDHAR6 was purified using a StrepTrap column (GE Healthcare) as previously reported (Johnston et al., 2015). Recombinant GSTU24 and GSTU25 were also purified using a Glutathione Sepharose 4B resin (GE Healthcare) as previously reported (Gunning et al., 2014). The remaining recombinant GSTs and OPRs/ONR were purified using a HisTrap column (GE Healthcare). GST bacterial cell pellets were resuspended in PBS, pH 7.4 whereas OPR/ONR bacterial cell pellets were resuspended in 50 mM potassium phosphate, pH 7.5. Recombinant proteins were eluted off the column using a gradient up to 500 mM imidazole.

2.5 DNAN PHYTOTOXICITY STUDIES

Sterile, stratified Arabidopsis seeds were germinated for 24 hours on 1/2 MS agar (Murashige and Skoog, 1962). Eight seedlings were transferred to shake flasks with 20 mL 1/2 MS media plus 1 % sucrose. Flasks were incubated on a rotary shaker at 100 rpm at 21 °C in 20 $\mu\text{mol m}^{-2} \text{s}^{-1}$ light with a 16-h photoperiod. After two weeks, media was replenished and dosed with either 0, 50, 125 or 250 μM of xenobiotic dissolved in DMSO. Controls that had not been dosed with xenobiotic were spiked with the equivalent concentration of DMSO. Seven days post-dosing, tissue was collected, washed and weighted. During the 7-day duration of the experiment (after dosing with xenobiotic), media samples were taken daily and quantified using HPLC analysis.

2.6 HPLC ANALYSIS

Reactions were analyzed by HPLC using a Waters HPLC system (Waters 2695 separator and Waters photodiode array detector) with a Waters X-Bridge C18 column (300 \times 4.5 mm, 5 μm). The mobile phases for the gradient conditions were as follows: mobile phase A, acetonitrile; mobile phase B, water plus 0.1% (v/v) formic acid. The gradient ran as follows: 0 min, 5% A and 95% B; 5 min, 5% A and 95% B; 25 min, 40% A and 60% B; 30 min, 100% A and 0% B; and 35 min, 5% A and 95% (v/v) B.

2.7 METHANOL EXTRACTS

Fresh plant tissues were ground in liquid nitrogen, and metabolites were extracted using 1 mL 10 mg^{-1} fresh weight methanol. After centrifugation, the supernatant was collected, evaporated, and resuspended in methanol:water (60:40) at a concentration of 1 $\mu\text{L mg}^{-1}$ fresh weight. Extracts were analyzed with HPLC.

2.8 MDHAR6 ACTIVITY ASSAYS

The activity of MDHAR6 towards DNAN and TNT was confirmed through the oxidation of NADH, monitored at 340 nm. Reactions contained 74 $\mu\text{g/ml}$ MDHAR and 100 μM NADH in 50 mM Tris, 1 mM EDTA (pH 7.6) and 10 % DMSO. Reactions were initiated with the addition of 500 μM TNT or DNAN.

2.9 SOIL STUDIES

The soil studies were conducted as previously described (Gunning et al., 2014; Rylott et al., 2011b). Briefly, five 5-day-old seedlings were planted into pots containing soil contaminated with a specified concentration of DNAN. Seedlings were then grown with $180 \mu\text{mol m}^{-2} \text{s}^{-1}$ light with a 12-hour photoperiod. Temperatures were set to 21 °C during light and 18 °C during dark temperatures. After five weeks of growth, aerial tissue was harvested and weighted.

2.10 HYDROPONIC EXPERIMENTS

A hydroponic experiment was established to determine the location of xenobiotic within Arabidopsis plants. Sterile seedlings were stratified and grown on $\frac{1}{2}$ MD agar for 10 days. These were then transferred to sponges cut into 2 by 2 cm sponges cut along the radius and inserted into corresponding cutouts in polystyrene rafts. Rafts, each containing six sponges, were floated in tip boxes containing 200 mL $\frac{1}{2}$ MS. These were incubated in high light with media was replenished weekly. After four weeks of incubation, boxes were dosed with xenobiotic dissolved in DMSO. Negative controls were spiked with the equivalent concentrations of DMSO. Plants were harvested four-day post-dosing. Roots and shoots were separated, washed and weighted before methanol extractions were performed.

2.11 TRANSCRIPTOMICS ANALYSIS

Arabidopsis seedlings were incubated in shake flasks containing $\frac{1}{2}$ MS growth media for 14 days and then dosed for six hours with 0, 60, 120, 240 or 480 μM DNAN. Five biological replicates were performed for each treatment. The RNA was harvested from plant tissue that had been ground in liquid nitrogen using EasyPure plant RNA kits (Transgen Biotech) and assessed using TapeStation (Aligent) gel-capillary electrophoresis. Levels of RNA degradation were found to be minimal, and the quantity of RNA sufficient for sequencing. Consequently, polyA tail selection was performed to enrich for messenger RNA (mRNA), and these samples sequenced using an Illumina HiSeq 3000 platform. The resultant 370 million pair-end fragments were mapped to the TAIR 10 Arabidopsis cDNA reference library (Berardini et al., 2015), and counts per million (CPM) values calculated to describe the abundance of each transcript by mapped reads scaled to fragments sequenced. Filtering was applied to the expression matrix to include only sequences present at over ten CPM in at least three biological replicates. This filtering reduced the number of transcripts in consideration from 33,602 to 14,186. Genes were annotated using classification provide by The Gene Ontology Consortium (2018), and gene families were obtained from TAIR (<https://www.arabidopsis.org/browse/genefamily/index.jsp>).

2.12 OPR ACTIVITY ASSAYS

Activity was determined by measuring oxidation of NADPH on a spectrophotometer at 340 nm. Reaction conditions were as follows: 50 mM potassium phosphate buffer (pH 7.5), 120 μM TNT/DNAN and 200 μM NAD(P)H. Reactions were initiated by addition of 50 μL protein to the cuvette, made up to a total of 1 mL.

2.13 GLUTATHIONE TRANSFERASE ACTIVITY

Purified recombinant GSTs were assayed against 1-chloro-2,4-dinitrobenzene (CDNB) to confirm the enzymes were active. Reactions were set up and spectrophotometrically measured at 340 nm as previously reported (Gunning et al., 2014).

Purified recombinant GSTU1, 2, 4, 7, 9, 19, 22, 24 and 24 enzymes were assayed for conjugation activity against DNAN. Reaction conditions were as follows: 100 mM potassium phosphate (pH 7.0), 5 μ M GSH and 0.2 μ M TNT/DNAN. Each reaction also contained 400 μ g/mL of each GST enzyme. Reactions were stopped by mixing 80 μ L of reaction mixture with 20 μ L 50% trichloroacetic acid. Precipitates were removed by centrifugation and the remaining supernatant analysed by HPLC. GSTU5, 16 and 24 were also assayed for conjugation activity on NTO. Reaction conditions and HPLC analysis was carried out as for other GST activity on DNAN.

2.14 STATISTICAL ANALYSIS

Differential gene expression analysis was performed using R package, EdgeR (Robinson et al., 2010). The expression matrix was normalized for depth and composition, and a general linear model was applied to calculate the number of significantly up/down-regulated transcripts. Genes were considered to be differentially expressed with a high degree of confidence with a P-value < 0.001 for the DNAN analysis and P-value < 0.05 for the NTO analysis.

One-way analysis of variance (ANOVA) tests and students t-tests where indicated were performed using R base packages. Data assessed by ANOVA was further tested for homogeneity of variance using Levene's test and data with $P < 0.05$ was followed by Tukey's post hoc test. * $p < 0.05$, ** $p < 0.01$, *** $p < 0.001$, **** $p < 0.0001$.

3.0 RESULTS AND DISCUSSION

3.1 TASK 4. – ESTABLISHING THE MECHANISM OF DNAN AND NTO TOXICITY

We first decided to establish how toxic DNAN was to Arabidopsis through agar plate experiments. Arabidopsis seeds, that had been chlorine gas sterilised were placed in rows on plates containing ½ MS agar and stratified for at least two nights at 4 °C, before being placed, upright, in a growth room. Arabidopsis grown in the presence of over 7 µM of DNAN had significantly shorter root lengths compared to the undosed plants (Figure 2). Moreover, under equivalent conditions of TNT, a more extreme phenotypic effect was observed.

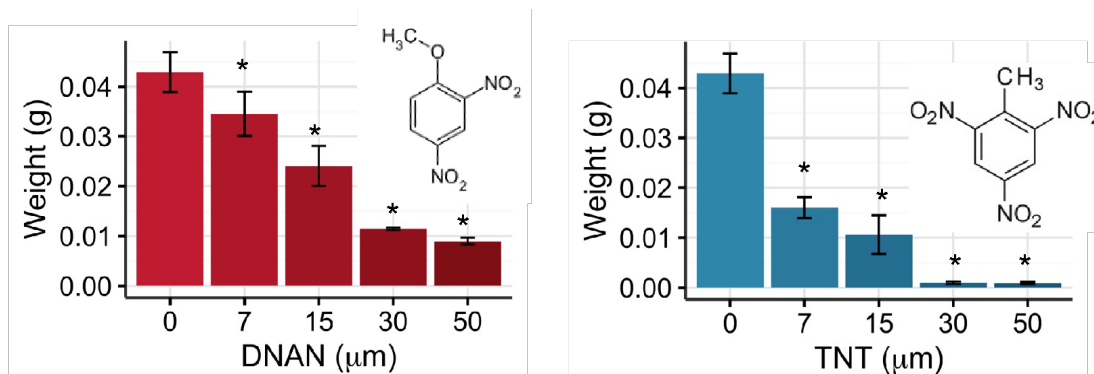


Figure 2. The Effect of Different Concentrations of (a) DNAN and (b) TNT on Growth of Arabidopsis Seeds (n = 48 ± SD).

Asterisks indicate a significant difference to the 0 µM controls (p < 0.05)

Soil studies were also performed to generate a toxicity curve of DNAN on plants. Concentrations of 100 mg/kg DNAN had little effect on root and shoot biomass. 250 mg/kg DNAN caused significant loss of both root and shoot biomass and plants could barely grow at all on 500 mg/kg DNAN. These data indicate that DNAN is likely toxic to plants at concentrations exceeding 100 mg/kg.

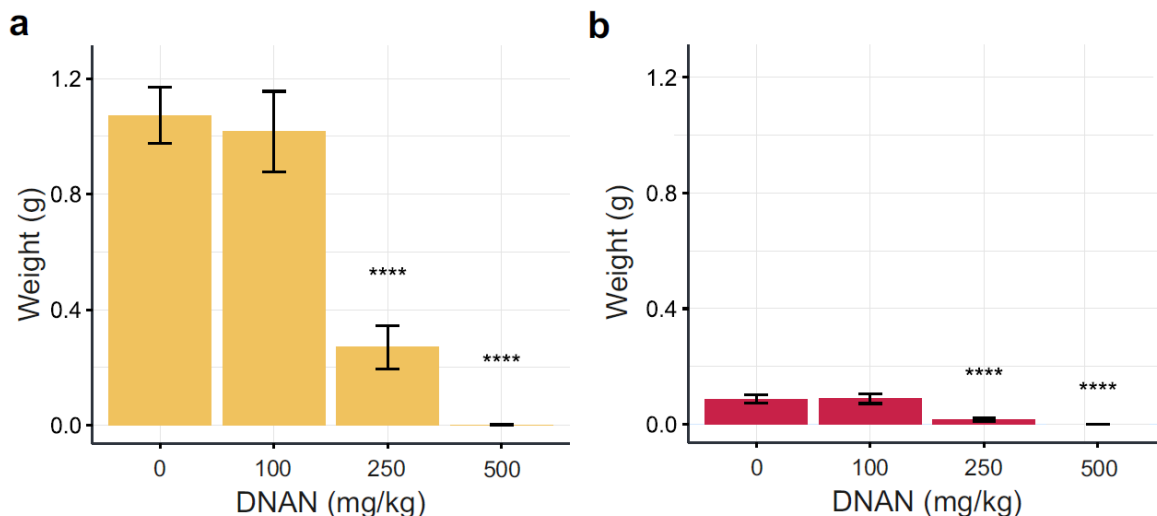


Figure 3. The Effect of DNAN on Arabidopsis Plant (a) Shoots and (b) Roots.

*Plants were grown in Soils dosed with the indicated concentrations of DNAN ($n = 40 \pm SD$). Asterisks indicate significant differences to the 0 μM control. **** $p \leq 0.0001$*

NTO and its reduction derivative ATO have been shown to have mild toxicity towards methanogenic bacteria, invertebrates and vertebrates (Lent et al., 2020; Madeira et al., 2018). As for DNAN, we carried out the same agar plate experiments in order to determine the toxicity of NTO on Arabidopsis plants (Figure 4). Note that NTO is a strong acid so the pH was maintained at 5.7. Significantly shorter root lengths were observed in 600 μM NTO conditions.

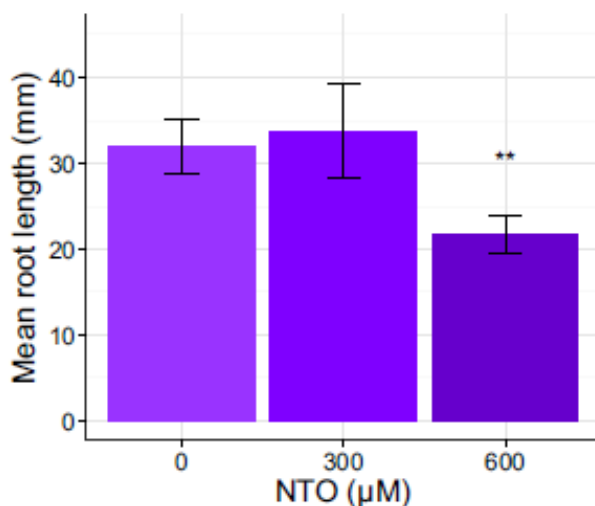


Figure 4. The Effect of Different Concentrations of NTO on Root Growth of Arabidopsis Seeds ($n = 27, 29$ and 24 for $0, 300$ and $600 \mu M$ NTO Respectively, $\pm SD$).

*Asterisks indicate a significant difference to the 0 μM control. ** $p < 0.01$.*

3.1.1 Task 4.1 Screening mutant Arabidopsis populations on media with DNAN and NTO

3.1.1.1 *T-DNA insertion libraries*

In addition to considering mutants lines known to play a role in xenobiotic toxicity, we performed undirected mutant screens using a Transfer-DNA (T-DNA) insertion induced collection of 6,868 confirmed homozygous mutants (N27941) from the Nottingham Arabidopsis Stock Centre (NASC) (Alonso et al. 2003).

To identify if these mutants had a phenotypic effect in the presence of DNAN, we set up screens at concentrations of 50 μ M DNAN in 1/2 MS agar in 6-well cell culture plates (Figure 5). This concentration was chosen as it had previously been seen to be sufficient to inhibit primary root growth in Arabidopsis. To aid high-throughput processing of these mutants, plants were visually assessed and given a mark out of one to five, where one represented the plants with the most severe phytotoxicity. Scoring was performed after fourteen days of growth, and the distribution of fitness scores is shown in Table 1.



Figure 5. (a) Arabidopsis Seedlings after Fourteen Days of Growth on 1/2 MS Media Containing 50 μ M of DNAN. (b) Plant Phenotypes Proscribed a Particular Fitness Score.

Table 1. Fitness Scores for Mutant Arabidopsis Libraries.

The lowest score (1) represents no germination and the highest (5) plants with the best growth.

Fitness score	Count
1	881
2	1827
3	2557
4	1094
5	155

Mutants with scores between two and four were not considered for further analysis as we considered these similar to wild type response. Mutants with fitness scores of 5 were considered for further study and were grown on solid agar with concentrations of either 0 or 50 μ M DNAN. After ten days of growth, root length was measured for 10 seedlings in each condition (Figure 6).

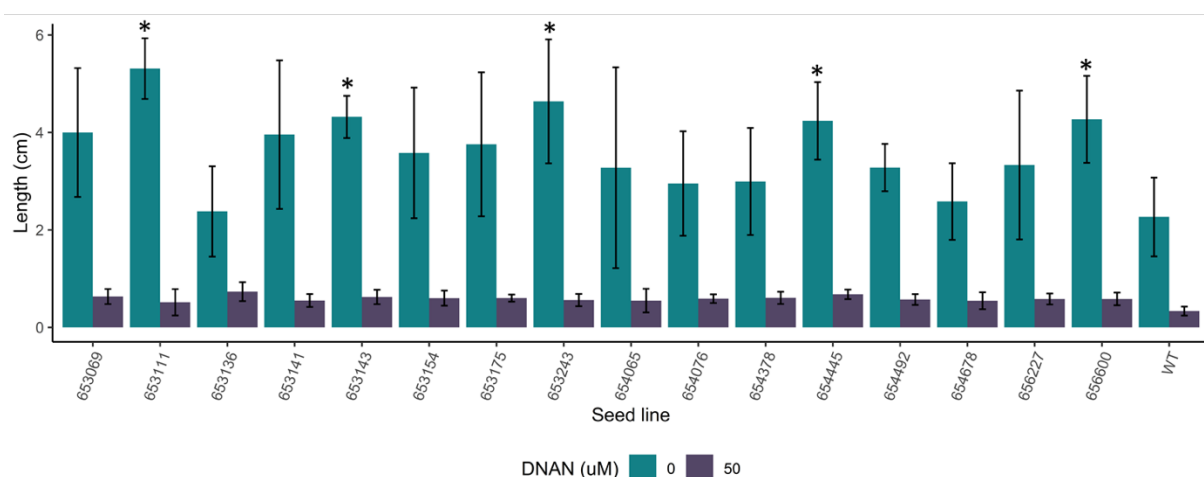


Figure 6. Root Length of Mutant Arabidopsis Lines Grown on Solid Agar with Either 0 or 50 μ M DNAN.

Roots were measured after ten days of growth. Bars represent the mean of ten Arabidopsis roots, and error bars represent the standard deviation of these means. Asterisks denote plants that significantly differed from the wild type in 0 μ M DNAN conditions.

Sixteen mutant lines showed a significant difference from wild type in the 50 μ M DNAN concentrations (Table 2), though five mutants also grew significantly better than wild type in no DNAN conditions. However, it should be noted that as seed for the mutant lines was generated by NASC, we did not have wild type seeds of equivalent age.

Of the 155 lines which showed enhanced growth in the presence of DNAN (Table 1), none contained mutations in genes known to be involved in xenobiotic detoxification (Ramel et al., 2012), despite the fact that a number of these genes were represented in the initial screen.

For example, we have demonstrated, through *in vitro* assays with heterologously produced protein, that oxophytodienoate reductases (OPR) can catalyze the nitroreduction of DNAN. However, mutant lines for OPR1 and OPR2 show no significant difference in root length when grown on 0, 7.5 or 15 μ M DNAN. This lack of observable phenotype is likely due to the redundancy in both the xenobiotic detoxification strategy and the enzymes that govern them.

Table 2. NASC ID of Mutant Lines that Grew Significantly Better than Wild Type in the Presence of DNAN.

Descriptions were obtained from TAIR. Fold change describes the difference in the transcription of these genes between 0 and 480 μ M conditions after six hours of exposure in liquid cultures.

Seed no.	Gene	Description	Fold change
653069	At3g07090	PPPDE putative thiol peptidase family protein	1.167847911
653111	At1g22730	MA3 domain-containing protein	1.2113364
653136	At4g29130	hexokinase 1	0.743979874
653141	At1g05500	Calcium-dependent lipid-binding (CaLB domain) family protein	1.000574403
653143	At4g13020	Protein kinase superfamily protein	0.750898687
653154	At2g45540	WD-40 repeat family protein / beige-related	0.816968634
653175	At2g01270	quiescin-sulphydryl oxidase 2	1.063638081
653243	At5g35420	transposable element gene	0.583308736
654065	At5g15800	K-box region and MADS-box transcription factor family protein	1.225173056
654076	At1g23480	cellulose synthase-like A3	0.705329968
654378	At1g29620	Cytochrome C oxidase polypeptide VIB family protein	nd.
654445	At5g03680	Duplicated homeodomain-like superfamily protein	0.884200799
654492	At1g05300	zinc transporter 5 precursor	1.463862811
654678	At5g26980	syntaxin of plants 41	1.380822307
656227	At5g40330	myb domain protein 23	1.049591996
656600	At3g05155	Major facilitator superfamily protein	0.143925565

3.1.2 Task 4.2 Characterizing allelic mutant, overexpression and knock-down Arabidopsis lines

Mutant Arabidopsis lines with either enhanced or detrimental growth effects in the presence of 2,4,6-trinitrotoluene (TNT) were assessed for differential phenotypes in the presence of DNAN. Previous studies (funded by SERDP ER-1498) investigating the effect of TNT on Arabidopsis identified the co-localized mitochondrial and plastidial form of monodehydroascorbate reductase (MDHAR6) as a primary cause of toxicity, with *mdhar6* mutants exhibiting increased growth when exposed to TNT compared to wild type backgrounds (Johnston et al., 2015). Due to the similar chemical structure of DNAN and TNT, we hypothesized that a similar effect might be observed with DNAN. When grown on solid agar with $\frac{1}{2}$ MS media supplemented with either 30 or 50 μ M of DNAN, *mdhar6* mutants had longer root lengths and accumulated substantially more biomass when compared to wild-type plants (Figure 7). Thus, our studies confirm that MDHAR6 plays a role in DNAN toxicity.

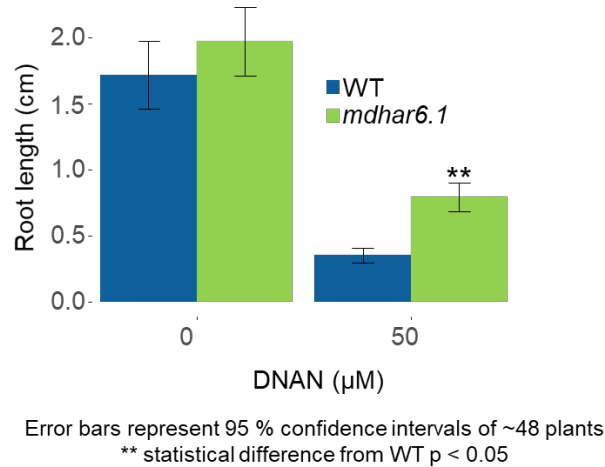


Figure 7. Arabidopsis root lengths of *mdhar6* mutants and WT seedling grown on solid agar with and without 50 μ M DNAN.

This experiment was replicated in soil studies, where *mdhar6* mutant plants performed significantly better than wild type, to the extent that no growth differences were observed between DNAN and no DNAN conditions (Figure 8). We have also tested mutant lines of other members of the MDHAR enzyme family: *mdhar1* and *mdhar3*. MDHAR1 is located in the matrix of the peroxisome, and MDHAR3 present in the cytoplasm of the cell. The growth and appearance of *mdhar1* and *mdhar3* were not significantly different from wild type plants. A mutant in *mdhar4*, which is targeted to the peroxisomal membrane (Lisenbee et al., 2005) will be tested shortly.

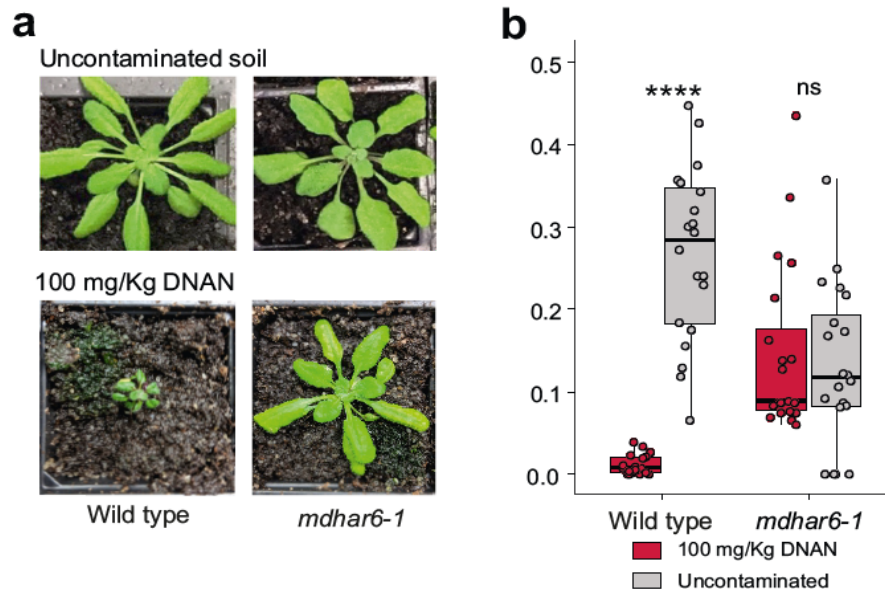


Figure 8. Six-week-old *mdhar6* Mutant and WT Plants Grown on 100 mg/kg Soil.

a - rosette weight of WT and *mdhar6* seedlings grown on soil for six weeks with 100 mg/kg DNAN and undosed soil. **b** - Six-week-old wild type (WT) and *mdhar6* Arabidopsis plants growing in soil contaminated with 100 mg/kg DNAN. Each treatment group consisted of 20 plants.

As MDHAR6 activity is known to be responsible for the majority of TNT phytotoxicity (Johnston et al., 2015), we tested its activity towards DNAN using recombinantly expressed, purified protein (Figure 9a). Activity of MDHAR6 towards DNAN was confirmed through the oxidation of NADH; however, at a markedly slower rate than that seen using TNT a substrate (Figure 9b). Reactions ran for 24-hours with a NADH recycling system confirmed that, like TNT, DNAN was not depleted, indicating that a futile cycle was being established (Figure 9c).

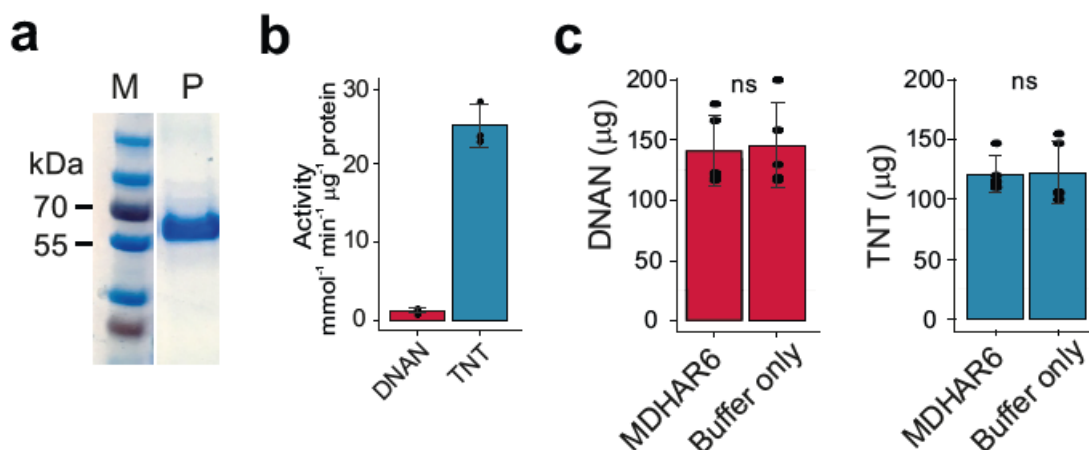


Figure 9. (a) SDS-PAGE Gel of Recombinantly Expressed, Purified MDHAR6 Protein. (b) Activity of MDHAR6 Activity on TNT and DNAN Substrate ($n = 3 \pm \text{SD}$). (c) Amount of DNAN and TNT Remaining in the Reaction after 24 Hours in the Presence of Enzymatic NADH-recycling System.

3.2 TASK 5. DETERMINING DEGRADATION INTERMEDIATES

3.2.1 Task 5.1 Measuring DNAN, NTO and transformation products using liquid cultures

The relative phytotoxicity of DNAN and TNT were compared using two-week-old liquid-culture-grown *Arabidopsis* plants dosed with a range of DNAN or TNT concentrations. TNT had the greatest phytotoxic effect at the highest (250 μM) concentration (Figure 10a-b) seven days after dosing, while a comparable effect was seen with both explosives at the mid-level (125 μM) concentration. Interestingly, at the lowest concentrations tested (50 μM), only DNAN significantly reduced ($P < 0.001$) fresh plant weight compared to the undosed control. Samples taken from the surrounding media revealed that while most of the TNT was rapidly removed within the first 24 hours, DNAN remained for considerably longer (Figure 10c). This prolonged exposure period results in the chronic toxicity seen in lower concentrations of DNAN.

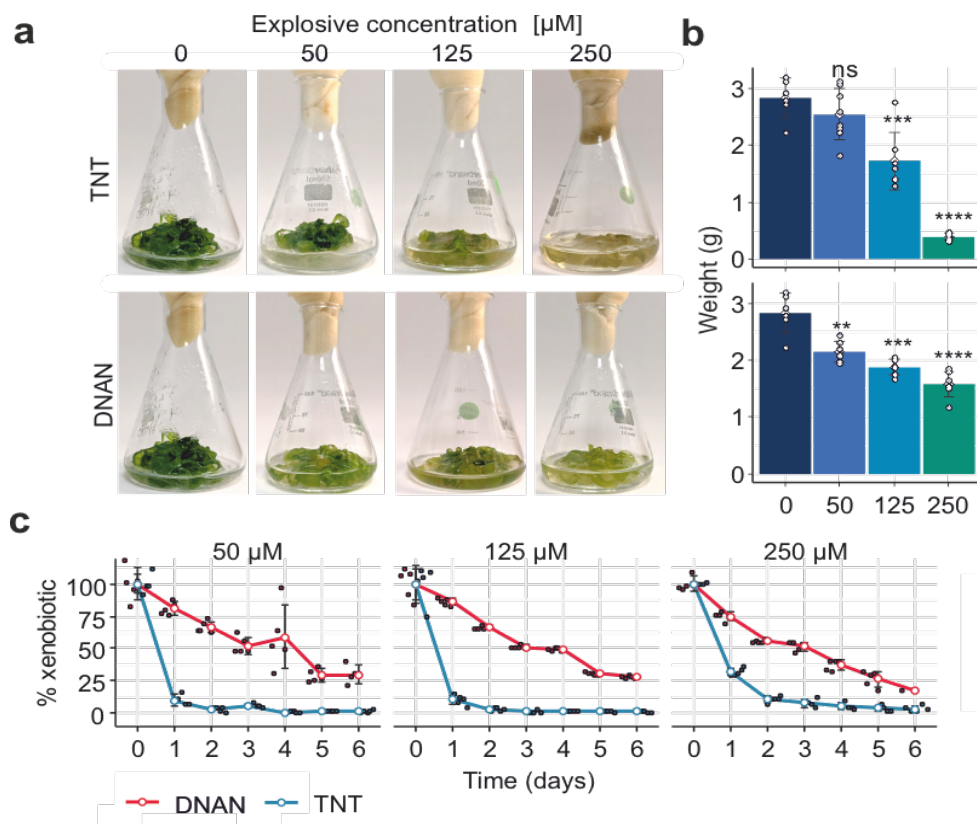


Figure 10. Phytotoxicity of DNAN and TNT on Arabidopsis.

(a) Appearance and (b) fresh weight of two-week-old *Arabidopsis* plants grown in shake flasks, seven days post-dosing ($n = 8$ plots \pm SD). (c) Depletion of explosive from shake flask media ($n = 5 \pm$ SD). The statistical significance, compared to no explosive, was performed by one-way analysis of variance followed by Tukey's post hoc test. $P < 0.05$ was considered as significant.

These data indicate a chronic toxic effect whereby, despite the plant showing less of an immediate toxic response to DNAN, a reduced ability to conjugate the compound results in a longer exposure period. The lower concentrations over a sustained period of time have a greater deleterious effect than comparable concentrations of TNT. To this effect, media samples, taken daily from each shake flask, and quantified through HPLC analysis, demonstrated a diminished percentage removal of DNAN compared to TNT throughout the time course. Additional peaks were observable throughout the TNT time course that likely correspond to transformation products, including hydroxyamino and amino products, and TNT-conjugates.

Tissue from seedlings that had been dosed with 250 μM DNAN were methanol extracted after four and seven days of growth. When plant tissue was examined, amino derivatives were identified (Figure 11a). The amount of amino derivative 2ANAN, (2-amino-4-nitroanisole; 2-methoxy-5-nitroaniline) was present at twice the concentration of DNAN within the tissue. This suggests that the conversion of DNAN to 2ANAN is a key step in DNAN detoxification. The reduction of the nitro-group predominantly occurs at the ortho position. This is expected and has been seen to be the favourable site of reduction during the bacterial transformation of DNAN (Olivares et al., 2013). It is also clear that multiple other peaks begin to appear in the tissue samples that are likely to represent transformation derivatives of DNAN (Figure 11b).

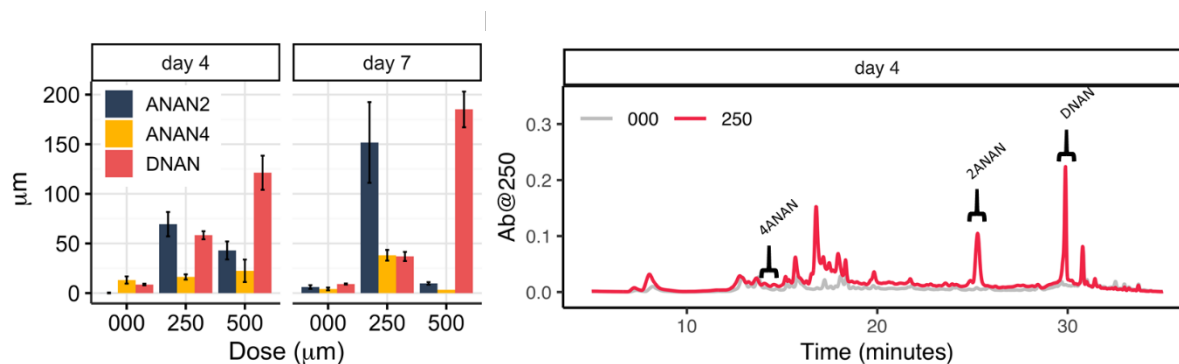


Figure 11. A) DNAN and Nitro-reduced Derivates within Arabidopsis Tissue 4 and 7 Days Post Dosing. (B) Chromatogram of Tissue Extracts from Arabidopsis Dosed with 250 μM of DNAN Compared to the Undosed Control.

DNAN and 2ANAN peaks are apparent in the xenobiotic dosed plant, as are a multitude of undefined peaks.

3.2.1.1 2ANAN

Therefore, it is important to consider how toxic 2ANAN is to Arabidopsis. Very little has been published on the toxicity of this compound though nitro-reduced products have been reported as less toxic in zebrafish (Olivares et al., 2016b) and microbes (Liang et al., 2013). To assess the phytotoxicity of 2ANAN, shake flasks, in the same set up as described above, as well as root length experiments were set up. Seedlings for root length experiments were germinated horizontally on plates containing ½ MS agar and were dosed with either 2ANAN, its para ortholog 4ANAN, the double nitro-reduced form DAAN, or the parent compound DNAN. After ten days of germination and growth, roots were weighed and measured.

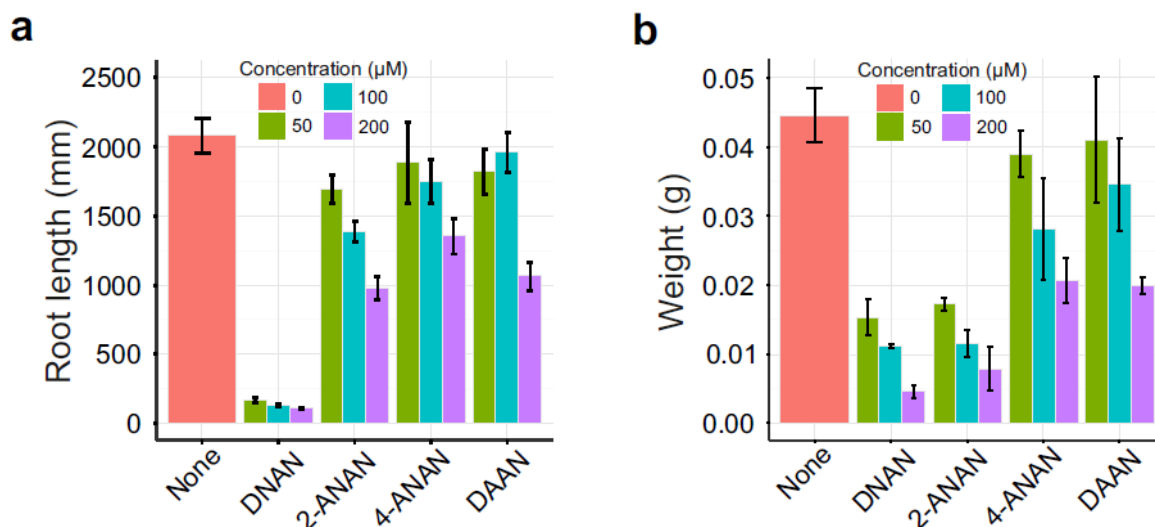


Figure 12. Effect of Different Concentrations of DNAN and Its Amino Derivatives on Arabidopsis (a) Seedling Root Length ($n > 24 \pm SD$) and (b) Seedling Biomass ($n = 3 \pm SD$).

These experiments had conflicting results. While root length was far less inhibited in the 2ANAN conditions compared to DNAN (Figure 12a), the mass of the plants was significantly reduced (Figure 12b), and the rosette growth appeared stunted. In shake flask conditions, however, the results are more in line with 2ANAN having a lesser phytotoxic effect, with no significant difference to the undosed control recorded in terms of weight, and 2ANAN depleting rapidly from the media. The differences between shake flask and agar experiments may be due to the different stages of development the plants were in at the time of exposure.

3.2.1.2 NTO

Phytotoxicity of NTO was also assessed on two-week-old liquid-culture-grown *Arabidopsis* plants. Experiments were set up as for DNAN and TNT, using a range of concentrations of NTO (Figure 13). 50 mM HEPES was added to the media to maintain pH 5.7, thus preventing NTO acidification. There was little difference in plant biomass up to 1000 μ M NTO, suggesting that NTO is not phytotoxic to plants at these concentrations.

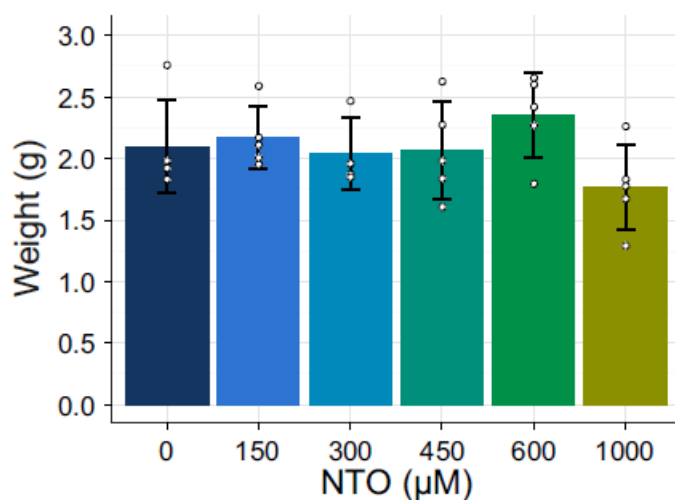


Figure 13. Fresh Weight of Two-week-old *Arabidopsis* Plants Grown in Liquid Culture, Seven-days Post Dosing.

One-way ANOVA and Tukey post-hoc test indicated no significant differences.

3.2.2 Task 5.2 Determining in-planta location of DNAN and NTO at the organ level

To determine the location of the xenobiotic within the plant, a hydroponic system was established. 10-day old seedlings were transferred into sponges that were placed in rafts, floating on 200 mL of $\frac{1}{2}$ MS media. These were then grown for a further two weeks before being dosed with either 250 or 500 μ M of DNAN or TNT. After four days, tissue from the roots and shoots were collected, washed and methanol extracted. The results are shown in Figure 14.

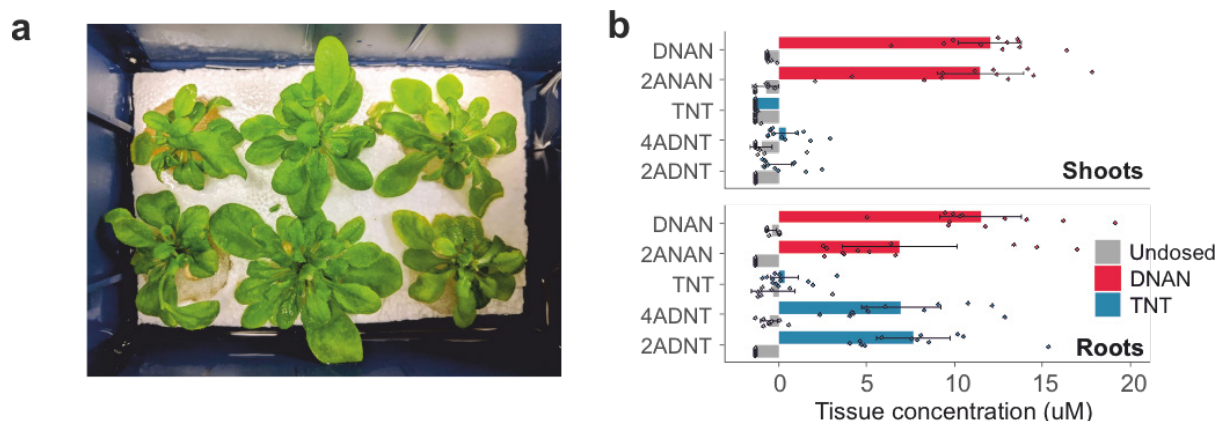


Figure 14. Location of Xenobiotic Compounds in Arabidopsis Plants.

(a) The hydroponic system. (b) concentrations of DNAN, TNT and intermediates within *Arabidopsis* tissue After dosing with 250 μ M explosive compound. ($n > 8 \pm SD$).

In the media from the plants dosed with TNT, 76 % and 74 % had been removed from the 125 μ M and 250 μ M TNT respectively. However, DNAN was not as readily depleted, with only 23 % and 12 % removal from the 125 μ M and 250 μ M treatments respectively.

Despite the significant differences between the uptake of TNT and DNAN, only DNAN could be detected within the root and shoot biomass, suggesting that TNT is more readily transformed by the plant (Figure 14b). Interestingly there was no peak corresponding to TNT detected within the roots, though its nitro-reduced products were present. In contrast, plants in boxes dosed with DNAN had some unknown peaks (~16 mins), but these were comparable to the DNAN peak. 2ANAN was also identified within the roots, though a higher concentration was present within the shoot.

3.3 TASK 6. BIOCHEMICAL PATHWAY CHARACTERIZATION

3.3.1 Task 6.1 Measuring gene expression in response to DNAN

Arabidopsis seedlings were incubated in shake flasks containing $\frac{1}{2}$ MS growth media for 14 days and then dosed for six hours with 0, 60, 120, 240 and 480 μ M DNAN. Five biological replicates were performed for each treatment. The RNA was harvested from the plants and assessed using TapeStation (Aligent) gel-capillary electrophoresis (Figure 15). Levels of RNA degradation were found to be minimal, and the quantity of RNA sufficient for sequencing (Figure 15). Consequently, polyA tail selection was performed to enrich for messenger RNA (mRNA), and these samples sequenced using an Illumina HiSeq 3000 platform. The resultant 370 million pair-end fragments were mapped to the TAIR 10 *Arabidopsis* cDNA reference library (Berardini et al., 2015), and counts per million (CPM) values calculated to describe the abundance of each transcript by mapped reads scaled to fragments sequenced. Filtering was applied to the expression matrix to include only sequences present at over ten CPM in at least three biological replicates. This filtering reduced the number of transcripts in consideration from 33,602 to 14,186.

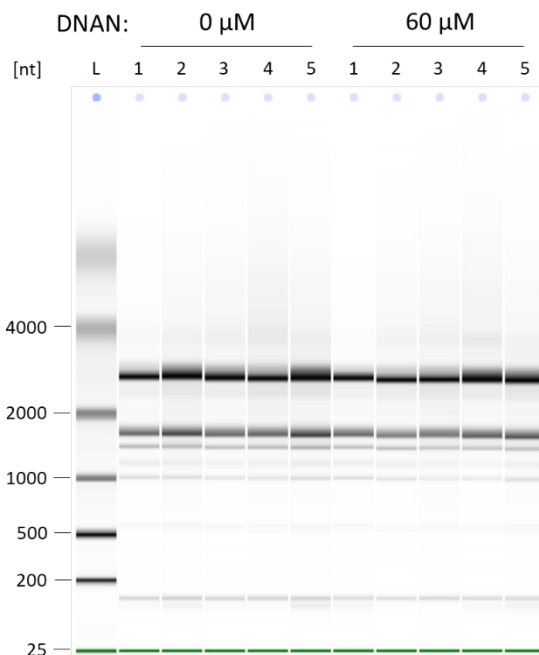


Figure 15. Electrophoresis Run Summary of the 0 μ M and 60 μ M DNAN Conditions.

Total RNA samples were assessed for quality on a TapeStation system. Ribosomal RNA peaks were consistently sharp and of the correct size throughout samples and a light smear was present in regions above 3000 nucleotides, suggesting the presence of intact messenger RNA. L – ladder; number – replicate.

EdgeR (Robinson et al., 2010), an R package for analysis of differential gene expression, was used to normalize for depth and composition, and a general linear model was applied to the matrix to calculate the number of significantly up/down-regulated transcripts. Genes were considered to be differentially expressed with a high degree of confidence with a P-value of under 0.001. Genes were annotated using classification provide by The Gene Ontology Consortium (Ashburner et al., 2000; The Gene Ontology Consortium, 2019)

Table 3. Number of Genes Deferentially Expressed ($P > 0.001$) after 6 Hours of Exposure to DNAN Compared to Control Conditions.

Condition	Upregulated	Downregulated
60 μ M	6	2
120 μ M	114	61
240 μ M	333	198
480 μ M	2330	2308

The highest concentration of DNAN induced the most significant differential expression (Table 3). In total, between the 0 μ M DNAN and 480 μ M DNAN conditions tested, 2,330 transcripts were upregulated with a high degree of confidence ($P < 0.001$) (Figure 16).

In concordance with studies on other xenobiotic compounds, which broadly categorize detoxification into three stages, including the activation of the compound by oxidation, reduction or hydrolysis; its conjugation; and the active transport of resultant compound (Ramel et al., 2012), genes with the highest upregulation included those involved in nitroreduction, conjugation and transport (Figure 17).

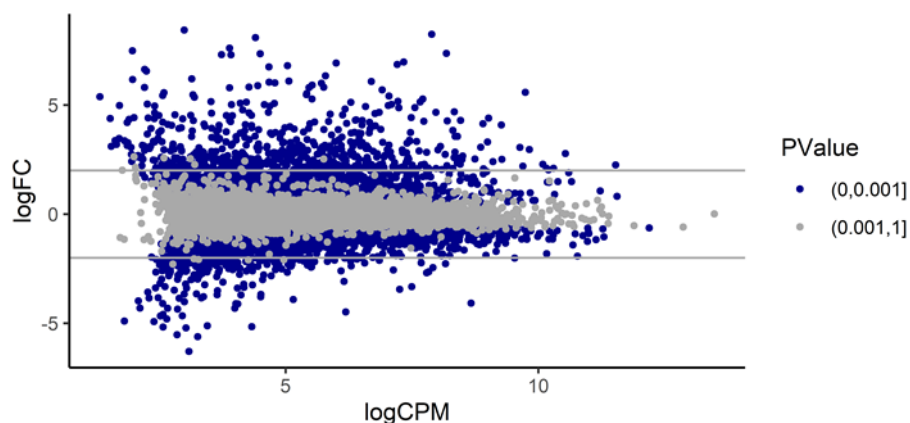


Figure 16. Differential Expression of Arabidopsis Transcripts in the Presence of 480 μ M DNAN.

Each point represents a gene and its response to DNAN. Dots colored blue show a significant difference ($P < 0.001$) in expression compared to no DNAN controls.

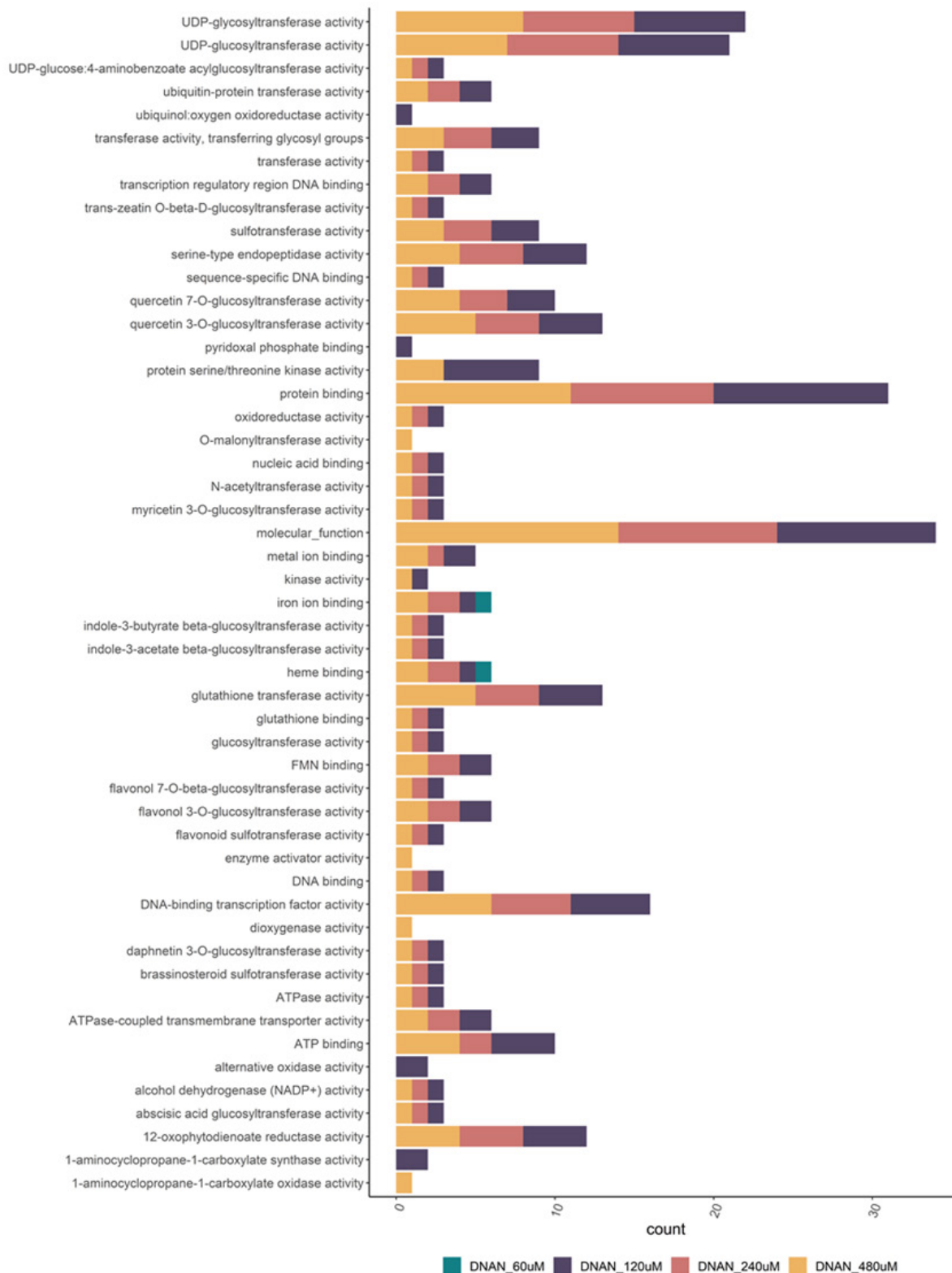


Figure 17. Gene Ontology (GO) of Genes Upregulated in Response to DNAN.

Genes were considered significantly upregulated at $P > 0.001$.

3.3.1.1 Glutathione S-transferases

The addition of a hydrophilic conjugate to a xenobiotic compound, like a glutathione or sugar moiety, decreases the parent compound's hydrophobicity. This conjugated form is unable to cross biological membranes via diffusion passively and allows active transportation to, and sequestration by, less active organelles. We have previously demonstrated that GSTs detoxify TNT through conjugation with glutathione (Gunning et al., 2014). In the case of TNT, this step alleviates phytotoxicity by physically separating the xenobiotic conjugate from the co-localized plastidial and mitochondrial form of monodehydroascorbate reductase (MDHAR6), a key determiner of phytotoxicity (Johnston et al., 2015).

Since glutathione-DNAN conjugation products have been described in Arabidopsis by (Schroer et al., 2017) we predicted that, like TNT, this conjugation could be catalyzed by GSTs alleviating DNAN phytotoxicity.

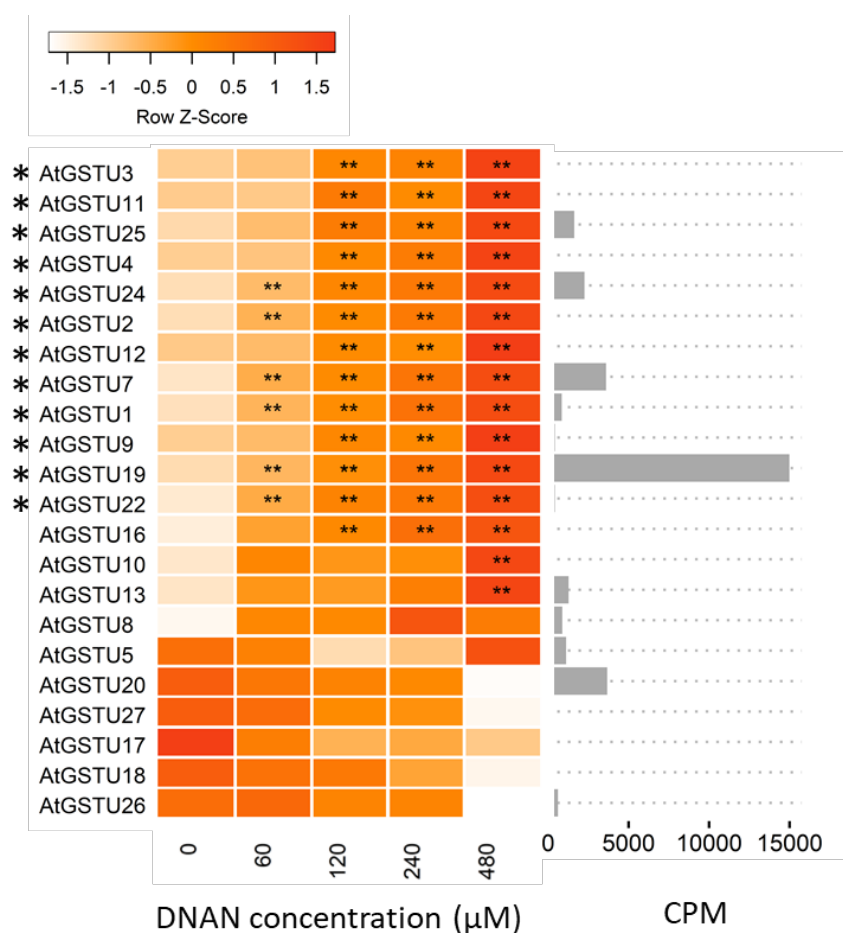


Figure 18. Abundance of Glutathione Transferase (GST) from the TAU Subfamily in Arabidopsis Plants Exposed for Six Hours to DNAN.

*Transcript abundance has been scaled across conditions. Single asterisks denote genes that have been cloned, expressed and purified, and tested for activity against DNAN. ** represents genes upregulated from undosed controls $P < 0.001$.*

Of the 39 GSTs present within our analysis, 17 were significantly upregulated between the lowest and highest DNAN concentrations (Figure 18). The TAU subfamily of glutathione transferases has been demonstrated to conjugate TNT (Gunning et al., 2014) and is the most upregulated family within our analysis. GST TAU 3 showed the highest fold change in expression, a 72-fold increase. The second largest change in expression level was GST TAU 11 with a 44-fold increase. However, overall expression levels of these transcripts were relatively low with CPMs of 16.4 and 29.8, respectively. When low expressing GSTs were excluded, i.e. expressing at less than 100 CPM, GST TAU 24 and GST TAU 25, both of which can conjugate TNT (Gunning et al., 2014), were most highly up-regulated. This indicates that these may instead have a more significant role in the detoxification of DNAN. Notably, GST U19 was also significantly more abundant than all the other GSTs in this analysis.

Since transcriptomic analysis suggests that glutathione transferases are involved in DNAN detoxification, we produced 11 upregulated GSTs in *E. coli* and purified the proteins to near homogeneity (Figure 19). In addition, GSTU3 and GSTU11 were also purified, however final purities was relatively poor (data not shown).

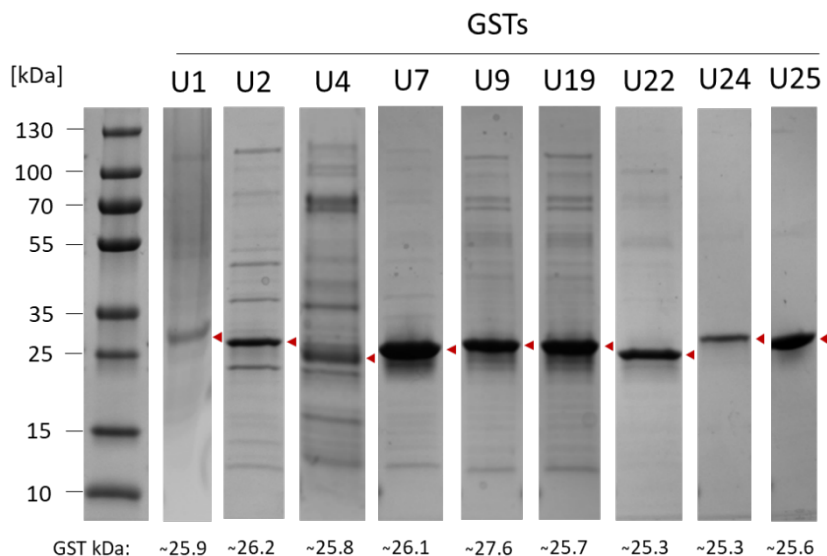


Figure 19. SDS-PAGE Analysis of the Recombinantly Expressed and Purified GSTs.

The relevant GST bands on the gel are indicated by the red markers. Theoretical molecular weights calculated by ExPASy ProtParam (Gasteiger et al., 2005) are indicated at the bottom of each lane.

The recombinant enzymes were confirmed as active by assaying for conjugation of 1-chloro, 2,4-dinitrobenzene (CDNB) to reduced glutathione (GSH) (Figure 20a). Next, the recombinantly produced enzymes were incubated with DNAN substrate, and the reaction products analyzed using HPLC (Figure 20b). In the conditions tested, which were sufficient to detect the conjugating activity of U19, U24 and U25 against TNT (Gunning et al., 2014), little to no activity was observed against DNAN, and no significant depletion of the parent compound observed.

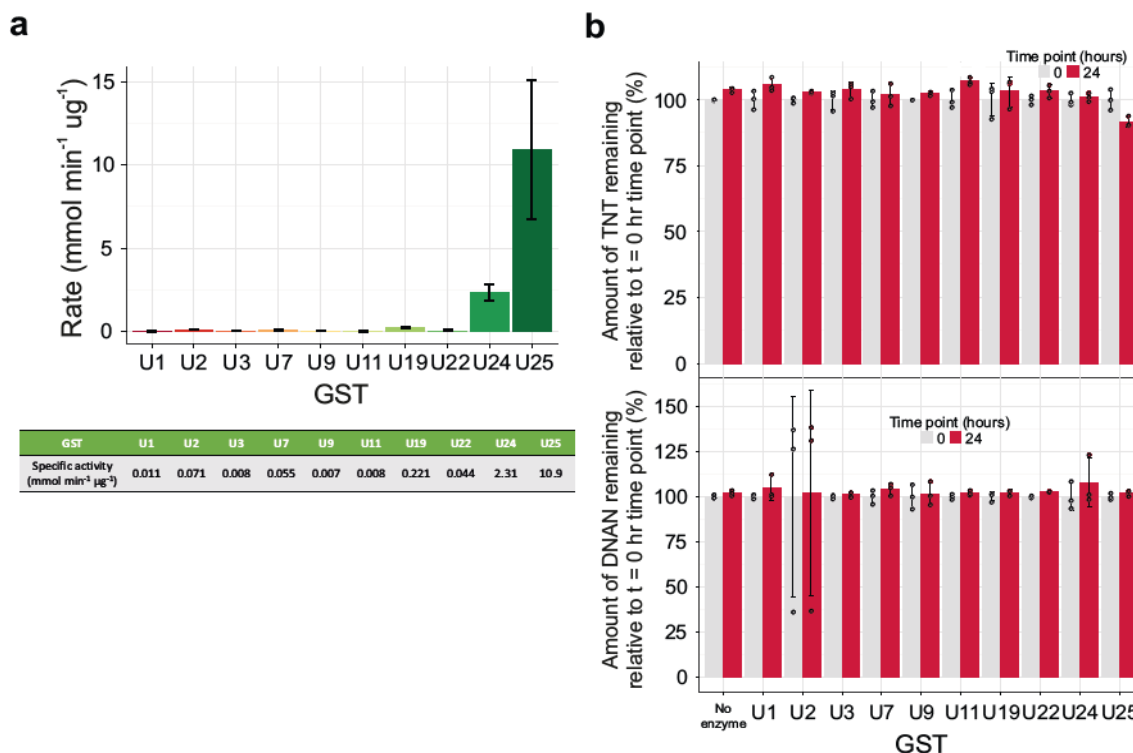


Figure 20. Activity of Recombinantly Produced GSTs on Substrate.

(a) Reaction rate of each GST on CDNB and GSH substrates to confirm each recombinant enzymes was active. Reactions contained 25 µg/mL of each recombinant GST was incubated with 5 mM GSH, 1 mM CDNB in 100 mM phosphate buffer. One-way ANOVA and Tukey post-hoc test indicated no significant differences. 6.5 ($n = 3 \pm SD$). (b) Change in amount of TNT/DNAN remaining after incubating with each GST and GSH substrate. Reactions contained 400 µg/mL of each recombinant GST, 5 mM GSH, 0.2 mM DNAN/TNT in 100 mM phosphate buffer pH 7.0. Reaction time points at 0 and 24 hours were taken and then analysed by HPLC. Concentrations were converted to amount of TNT/DNAN remaining by normalising each enzyme/control to the 0 hour time point ($n = 3 \pm SD$).

3.3.1.2 Uridine diphosphate-glycosyltransferases

Uridine diphosphate-glycosyltransferases (UGTs), like glutathione transferases, are known to be upregulated in response to TNT. UGTs aid detoxification through the attachment of an activated nucleotide sugar group to the xenobiotic (Gandia-Herrero et al., 2008; Ross et al., 2001). However, unlike GSTs, which can conjugate TNT directly, UGTs generally require hydroxyl, sulfhydryl, amino or carboxyl groups to act upon. Therefore, UGTs require molecules lacking these groups to be activated. In the case of TNT, this activation proceeds through nitroreduction, and our studies with heterologously produced UGTs have demonstrated that conjugation occurs to either hydroxylamino dinitrotoulene (HADNT) or amino dinitrotoulene (ADNT) derivatives (Gandia-Herrero et al., 2008).

Of the 107 Arabidopsis UGTs considered in this analysis, 21 were upregulated in the presence of DNAN compared to undosed controls (Figure 21). These included six genes (UGT73B4, UGT74E2, UGT73C1, UGT73C6, UGT73B2, UGT73B5) which can conjugate HADNT or ADNT isomers. Of these, UGT74E2 (AT1G05680) had the highest fold increase between DNAN and no DNAN conditions and was the third most upregulated protein within the entire transcriptome.

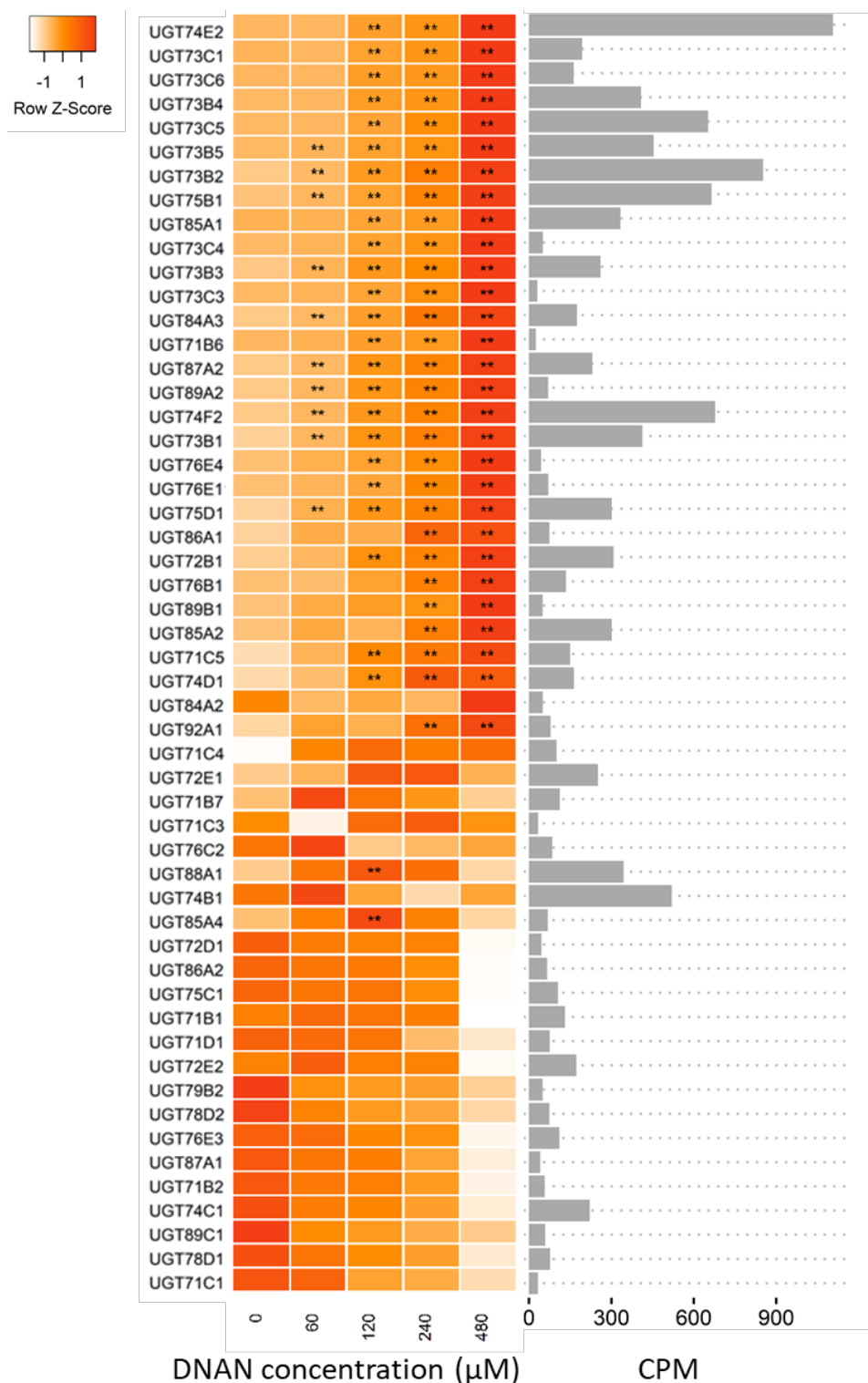


Figure 21. Abundance of Glycosyltransferase (UGT) Transcripts in Arabidopsis Plants across a Range of DNAN Concentrations.

*Genes in bold have been cloned, expressed and purified, and tested for activity against DNAN. ** represents genes upregulated from undosed controls $P < 0.001$.*

3.3.1.3 Oxophytodienoate reductases

If glycosyltransferases are capable of catalyzing the conjugation of DNAN in Arabidopsis as our analysis suggests, we would expect there to be increased expression of enzymes capable of activating the DNAN for glucose conjugation. Members of the oxophytodienoate reductases (OPR) family are good candidates for this activity, as they can catalyze the activation of TNT and are upregulated in the presence of DNAN.

The OPR family are homologs of the Old Yellow Enzyme (OYE) family, named because of the distinctive color of their flavin mononucleotide (FMN) cofactor. The OPRs, through the oxidation of NAD(P)H, reduce the nitro groups concurrently to nitroso- and hydroxyamino- (HADNT) intermediates and amino- (ADNT) products (Beynon et al., 2009). Interestingly, OPR1 (At1g76680) can follow an additional alternate pathway to produce dihydride- and hydride-Meisenheimer complexes (2H—TNT and H—TNT). Hydride-Meisenheimer complexes are of particular interest, as the destabilization of the ring structure through the inclusion of a nucleophile allows for further biotransformation to occur and potential downstream mineralization (Figure 22).

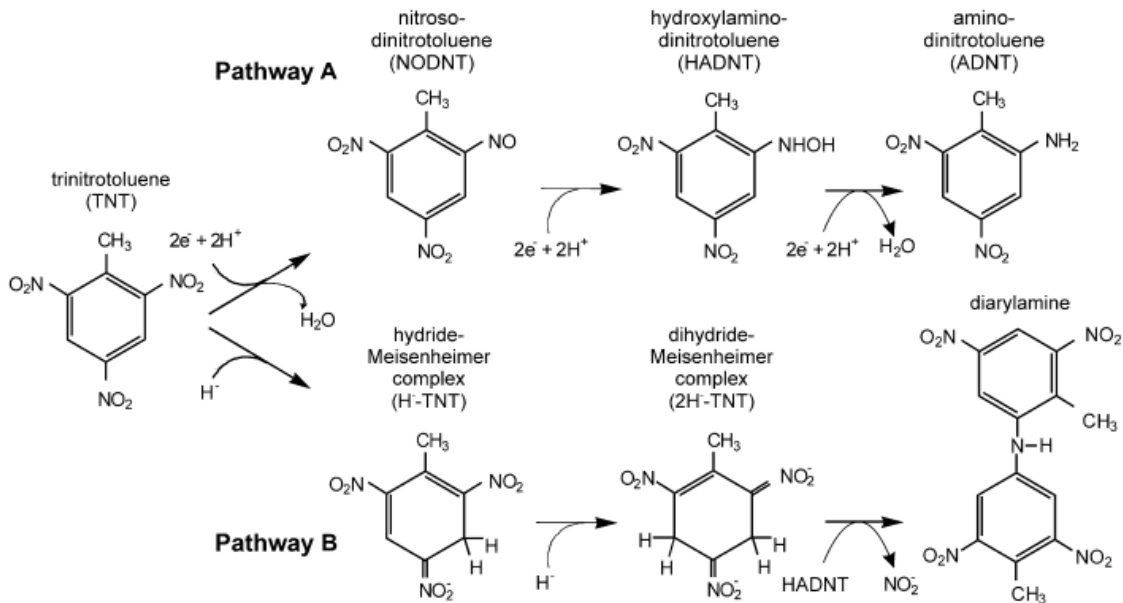


Figure 22. Transformation of TNT by oxophytodienoate reductases (OPR). Sourced from (Beynon et al., 2009).

In Arabidopsis, the OPR family consists of six genes, two of which, OPR4 (At1g17990) and OPR5 (At1g18020), are identical duplications of each other. OPR1, OPR2 (At1g76690) and OPR4/5, were upregulated in response to DNAN (Figure 23). OPR3 (At2g06050), required for the biosynthesis of jasmonic acid, and the only OPR with a defined role within Arabidopsis, did not differentially express, and OPR6 was not detected at levels high enough to be included in the analysis.

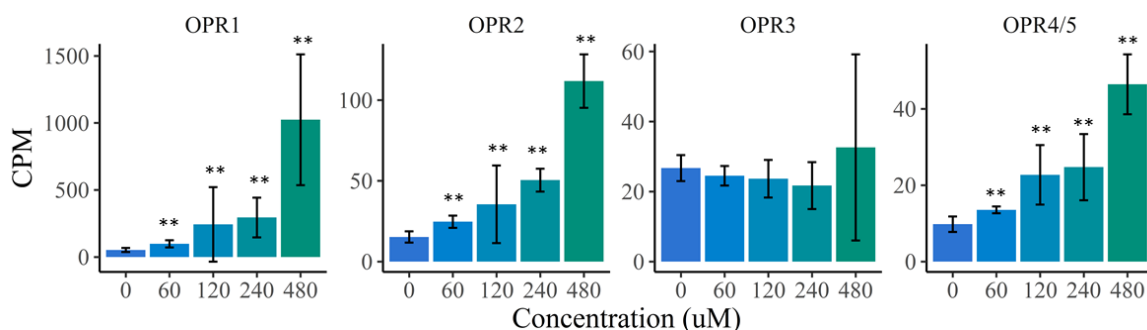


Figure 23. Counts per million (CPM) of Oxophytodienoate Reductases (OPR) Gene Responses to Varying Concentrations of DNAN.

Error bars represent the standard deviation of five biological replicates. ** represents genes upregulated from undosed controls $P < 0.001$.

We heterologously produced purified protein for OPR1 and OPR2 in *E. coli* and confirmed that they both catalyze the nitroreduction of DNAN (Figure 24). Alongside the OPRs, an *E. cloacae* pentaerythritol tetranitrate reductase (ONR) was also recombinantly produced and incubated with DNAN/TNT to act as a positive control. TNT and its transformation products are known to be located almost exclusively in the root tissues. However, in our localization studies, we observed that DNAN was present in the roots and shoots at comparable concentration, whilst 2ANAN was only in the aerial tissue of Arabidopsis. Since OPR1 and OPR2 are primarily associated with expression in root tissue, OPR4/5, which is preferentially expressed in aerial tissue, may catalyze the observed transformation of DNAN to 2ANAN. A role for OPR4/5 in xenobiotic detoxification would be significant as despite being structurally related to OPR1 and 2; it lacks a C-terminal region predicted to be involved in the binding of both the substrate and phosphate group of NADPH (Breithaupt et al., 2001). Therefore, we also recombinantly produced OPR4/5 and confirmed some minimal activity on DNAN.

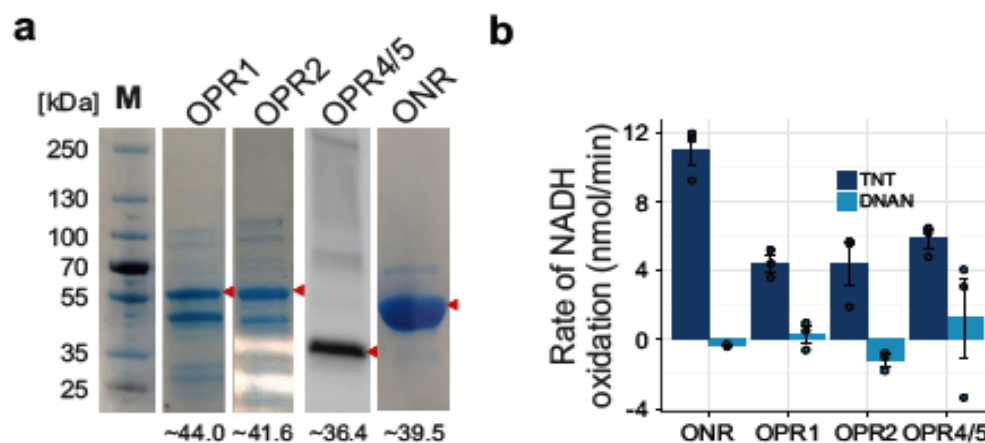


Figure 24. Recombinant Protein Production and Activity of the OPRs and ONR Control.

(a) SDS-PAGE analysis of recombinantly expressed and purified OPRs and ONR control. The relevant GST bands on the gel are indicated by the red markers. Theoretical molecular weights calculated by ExPASy ProtParam (Gasteiger et al., 2005) are indicated at the bottom of each lane. (b) OPR and ONR activity on DNAN and TNT substrates. Reactions contained 50 μ L protein, 120 μ M DNAN/TNT, 200 μ M NADPH in 50 mM potassium phosphate buffer, pH 7.5 ($n = 1 \pm$ SD).

3.3.1.4 OPR shake flask data

Alongside investigating the role of the OPRs *in vitro*, we have grown fresh seed from Arabidopsis 35S-OPR overexpression lines. Two-week-old Arabidopsis plants were dosed with TNT or DNAN. The depletion rate of the xenobiotic was measured over a one-week incubation, with plant biomass weighed at the end. Though we saw no significant difference in terms of plant biomass (Figure 25a), we observed subtle differences in the concentration of DNAN within the growth media (Figure 25b). Though the reduced concentration of DNAN was not statistically significant for 35S-OPR1 ($p = 0.089$), analysis of media at day 3 and 4 indicated a significant reduction in DNAN (data not shown). These data suggest that 35S-OPR1 plants have an increased ability to remove DNAN from the media, the only overexpression line to have a significant effect on DNAN concentration compared to wild type. Conversely, 35S-OPR2 lines exhibited a significant increase in the concentration of 2ANAN detected in the media.

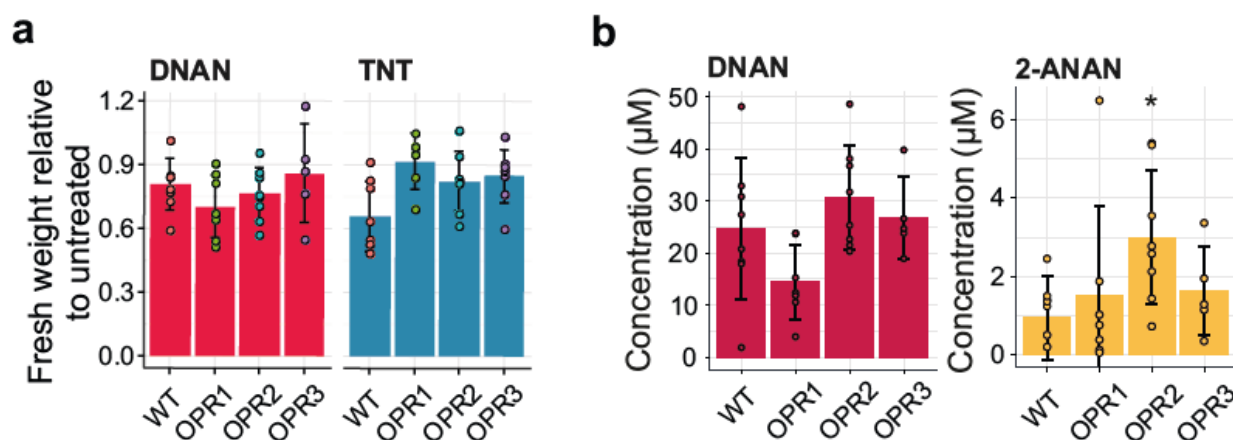


Figure 25. Growth of 35S-OPR Overexpressor Plant Lines in TNT or DNAN Dosed Media.

(a) Plant biomass after a one-week incubation in dosed media. Biomass was normalised against an untreated control ($n = 7 \pm SD$). (b) Concentration of DNAN and 2-ANAN remaining in the media after seven days ($n \geq 5 \pm SD$). Student's *t*-test was used to calculate significance. * $p < 0.05$.

3.3.1.5 Other enzyme families

Multidrug resistance-associated proteins (MRPs), from the subfamily C of ATP-dependent ABC transporters, have been identified as having a role in transporting glutathione conjugates across the tonoplast membrane into the vacuole (Klein et al., 2006; Lu et al., 1997). Five MRPs are upregulated in response to DNAN. AtMRP3 was most upregulated (16-fold) MRP in our analysis (Figure 26). However, rather than being part of subfamily C, AtMRP3 is in fact from classified as a subfamily G ABC transporter. This subfamily is not associated with glutathione transport or vacuolar transport, but instead implicated in resistance to lead metal in Arabidopsis (Lee et al., 2005). Moreover, AtMRP3 has also been confirmed to be an abscisic acid transporter (Kang et al., 2015).

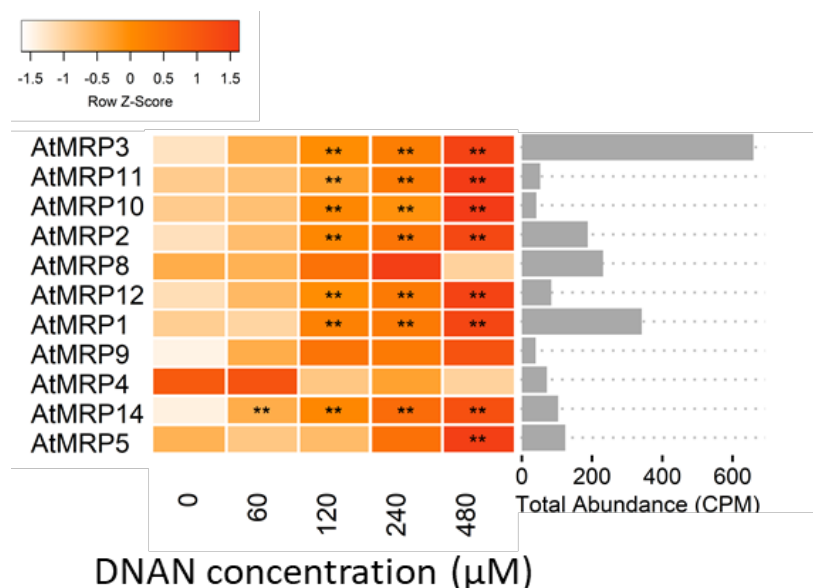


Figure 26. Abundance of Multidrug Resistance (MDR) Transcripts, from Subfamily C of ABC Transporters, Across a Range of DNAN Concentrations.

*Genes in bold have been cloned, expressed and purified, and tested for activity against DNAN. ** represents genes upregulated from undosed controls $P < 0.001$.*

Once inside the vacuole, glutathione conjugates may undergo further processing (Coleman et al., 1997). The gamma-glutamyl bond between Glu and Cys in glutathione can be cleaved by gamma-glutamyl transpeptidases (GGTs), of which there are four in Arabidopsis. Of these, GGT3 (AT4G29210) is the only enzyme located in the vacuole and has been demonstrated to remove the glutamate group from other conjugated xenobiotics (Ohkama-Ohtsu et al., 2007). However, GGT3 was not differentially expressed in our analysis (Figure 27).

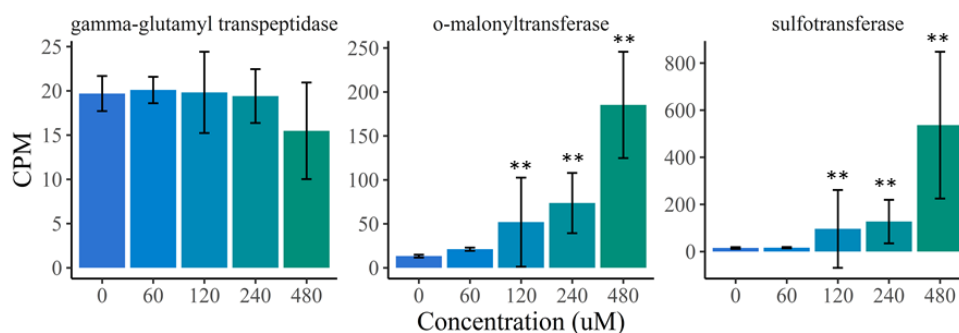


Figure 27. Counts per Million (CPM) of Gamma-glutamyl Transpeptidase (ggt3; AT4G29210), o-malonyltransferase (AT5G39050) and Sulfotransferase (AT2G03760) Gene Responses to Varying Concentrations of DNAN.

*Error bars represent the standard deviation of five biological replicates. ** represents genes upregulated from undosed controls $P < 0.001$.*

Glucoside conjugates are considered to be stored in the vacuole; however, it has been speculated that they can translocate out of the vacuole and be utilized for integration into the lignin fraction of root cell walls (Liu et al., 2011). However, incorporation into lignin is experimentally hard to verify due to the difficulty in extracting residues bound into the lignin macromolecule. Only a single gene, a cell wall-bound peroxidase (AT5G64120) known to be involved in cell wall remodeling, was upregulated in our transcriptomic analysis. Our findings for DNAN are in contrast to our earlier TNT study (Gandia-Herrero et al., 2008) and that of (Landa et al., 2010). Both studies reported upregulation of cell wall modifying genes within *Arabidopsis* roots after treatment with TNT. However, these disparate results may be indicative of the different time scales considered, and additional investigation will be required to confirm the physiological fate of DNAN.

Glucoside conjugates may also be further processed by malonylation. This has been reported to regulate the secretion of phenolic-glucoside to the extracellular space with the addition of a malonate group resulting in an increased accumulation of the xenobiotic in the cell (Taguchi et al., 2010). Though it is unclear whether malonylation plays a physiological role in DNAN detoxification, AT5G39050, which encodes an enzyme with O-malonyltransferase activity, was upregulated in the presence of DNAN. Other transferases were also upregulated in the presence of DNAN. This includes AT2G03760, an enzyme with putative sulfotransferase activity, that was upregulated 38-fold in the presence of 480 μ M DNAN (Figure 27).

3.3.1.6 *MRP2* root length assays

Our transcriptomic analysis indicated that MRP2 was significantly upregulated in the presence of DNAN. MRP2 encodes an ATP-binding cassette (ABC) transporter that has been associated with the transport of xenobiotics (Hoffmann and Kroemer, 2004). Therefore, we next screened a mutant line of MRP2 *Arabidopsis* plants. Seedlings were germinated and grown on $\frac{1}{2}$ MS agar containing either 0 or 20 μ M DNAN, and primary root lengths measured (Figure 28). Roots grew longer in the *mrp2* plant lines under 0 μ M DNAN conditions. Though primary root lengths were reduced in the presence of 20 μ M DNAN, no significant difference was observed between wildtype and *mrp2* plant lines.

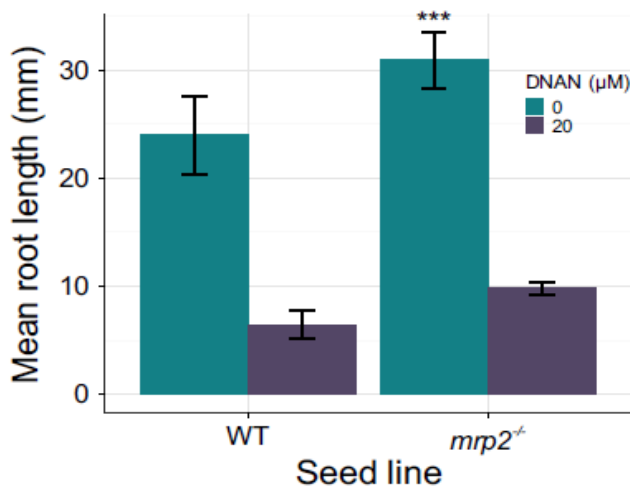


Figure 28. Root Length of Wildtype and *mrp2* Mutant *Arabidopsis* Lines Grown on Solid Agar with Either 0 or 20 μ M DNAN (in order of the Bars, Each Had n = 21, 18, 23 and 25 \pm SD). Student's t-test *** p < 0.001.

3.3.1.7 NTO transcriptomics

As NTO acts as a strong acid, it is severely detrimental to the germination and growth of *Arabidopsis* when the pH is not controlled. We have previously demonstrated that exposure of *Arabidopsis* to NTO in the presence of a buffering system using 4-(2-hydroxyethyl)-1-piperazineethanesulfonic acid (HEPES) had little effect on the phenotype of *Arabidopsis* seedlings in liquid culture and was sufficient to maintain the pH at 5.7 over a week long time course.

To investigate whether a gene regulatory response was elicited by *Arabidopsis* after exposure to NTO in these buffered conditions, we performed a transcriptomic analysis. One-day old seedlings were transferred into shake flasks containing $\frac{1}{2}$ M/S + 1% sucrose, buffered with 50 mM HEPES. Plants were grown in liquid culture for fourteen days before being dosed with 0, 300, or 600 μ M NTO for six hours and harvested by snap freezing in liquid nitrogen. After grinding plant material using a mortar and pestle, we were able to extract total RNA using Easypure plant RNA kits and the standard protocol. These samples were assessed for quality and quantity by capillary electrophoresis and found to be exemplary, allowing us to proceed with mRNA enrichment, cDNA synthesis, and library preparation before being passed onto an external company for sequencing.

After quality checks, the resulting reads were analyzed on the LINUX cluster by mapping each sample to the TAIR10 cdna (Lamesch et al., 2012) reference with BWA software. Counts per million mapped reads (CPM) were calculated, and the EdgeR R package was used to model gene counts using negative binomial distribution in order to perform differential analysis. Gene expression counts were normalized and filtered to include only tags which were expressed at higher than 5 CPM in at least five samples. A GLM was fitted to this normalized and filtered expression matrix. Using a p-value cut off of $P < 0.01$, 109 genes were significantly upregulated between 0 μ M and 600 μ M NTO conditions, while 87 genes were downregulated. Between the 0 μ M and 300 μ M NTO conditions, 112 genes were significantly upregulated, and 50 were downregulated. When the NTO conditions were given equal weighting within the GLM, 105 genes were significantly upregulated and 85 downregulated. The number of differentially expressed genes were far fewer than observed with our DNAN transcriptomic experiment, which used the same methodology and similar concentrations of xenobiotic, reflective of the more severe phytotoxic effect of DNAN.

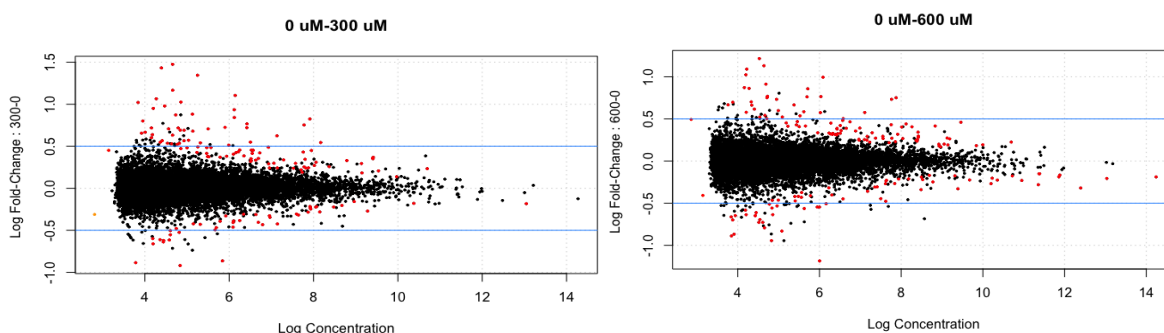


Figure 29. Differential Expression of *A. thaliana* Transcripts in the Presence of 300 and 600 μ M NTO.

Each dot represents a genes response to NTO. Genes coloured RED have a significant difference ($p < 0.01$) in expression compared to no compound controls.

Focussing on the genes upregulated between both conditions, three of the top genes (AT1G08430.1, AT2G04070.1, AT3G23550.1) were related to MATE efflux transporters. MATE efflux transporters, also known as the multidrug and toxic compound extrusion family, are known to export xenobiotics. AT2G04070.1 was in the top 50 proteins upregulated by TNT in an earlier microarray-based investigation (Gandia-Herrero et al., 2008). The same protein was also upregulated here in our DNAN investigation, alongside AT3G23550.1.

Plant defensins are cysteine-rich antimicrobial peptides which appear to be upregulated in the presence of NTO. Within the top ten upregulated proteins, two were plant defensins. These are typically associated with protection against fungal infection through the destabilization of the cell membrane of a pathogen. However, in more recent years, they have been implicated in conferring heavy metal tolerance in metal hyperaccumulators (Mirouze et al., 2006). Interestingly, transcriptomic analysis indicated that in the presence of DNAN, plant defensins were not upregulated.

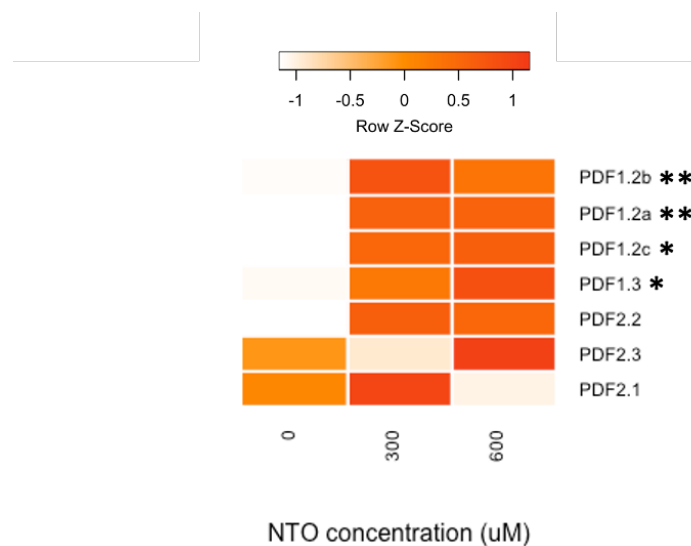


Figure 30. Abundance of Plant Defensin (PDF) Transcripts in Arabidopsis Plants across a Range of NTO Concentrations.

*** represents genes upregulated from undosed controls $P < 0.05$.*

Members of the glycosyltransferase family were also upregulated, including UDP-GLUCOSYL TRANSFERASE 73C6 which had the fifth-highest upregulation. The addition of a hydrophilic conjugate to a xenobiotic compound, such as a glutathione or sugar moiety, decreases the hydrophobicity of the parent compound. This conjugated form cannot passively diffuse across biological membranes and allows active transport to, and sequestration by, less active organelles. These came from the glycosyltransferase 1 and 35 families. AT5G61160.1 was upregulated in our analysis. This enzyme has homology to acetyltransferases involved in malonylation, which is associated with the regulation of the secretion of phenolic-glucoside to the extracellular space through the addition of a malonate group (Taguchi et al., 2010). We have previously seen glutathione transferases upregulated in response to DNAN and TNT. Three were upregulated in response to NTO, albeit with p values of $P < 0.05$.

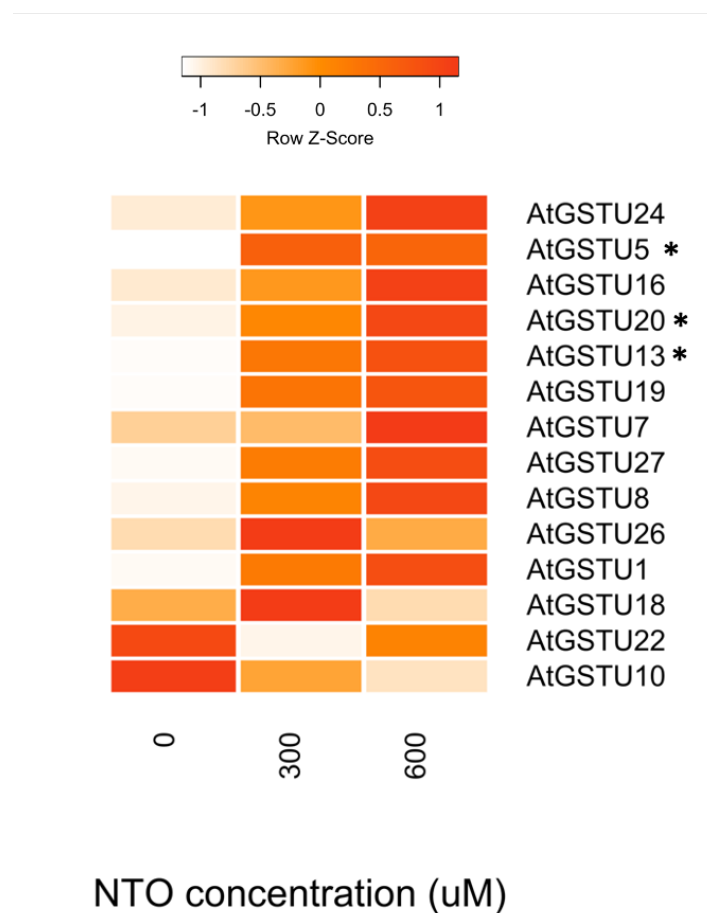


Figure 31. Abundance of Glycosyltransferase Transcripts in Arabidopsis Plants Across a Range of NTO Concentrations.

** represents genes upregulated from undosed controls $P < 0.05$.*

The cytochrome P450s were one of the most upregulated gene families. P450s were previously shown to be upregulated in Arabidopsis plants when exposed to TNT and RDX for 24 hours (Ekman et al., 2005). Our transcriptomic analysis for DNAN indicated these proteins were also upregulated. Ekman et al. described three cytochrome P450s that were upregulated by RDX, one of which (CYP71A20) was also upregulated by NTO in our analysis. In addition, Ekman *et al* identified that AT5G20150.1, an SPX domain-containing protein, was highly upregulated by RDX. This protein was also highly upregulated by NTO in our analysis. The role of AT5G20150.1 is not clear, though SPX domains have been characterized to be involved in nutrient signalling (Duan et al., 2008; Secco et al., 2012; Wang et al., 2008).

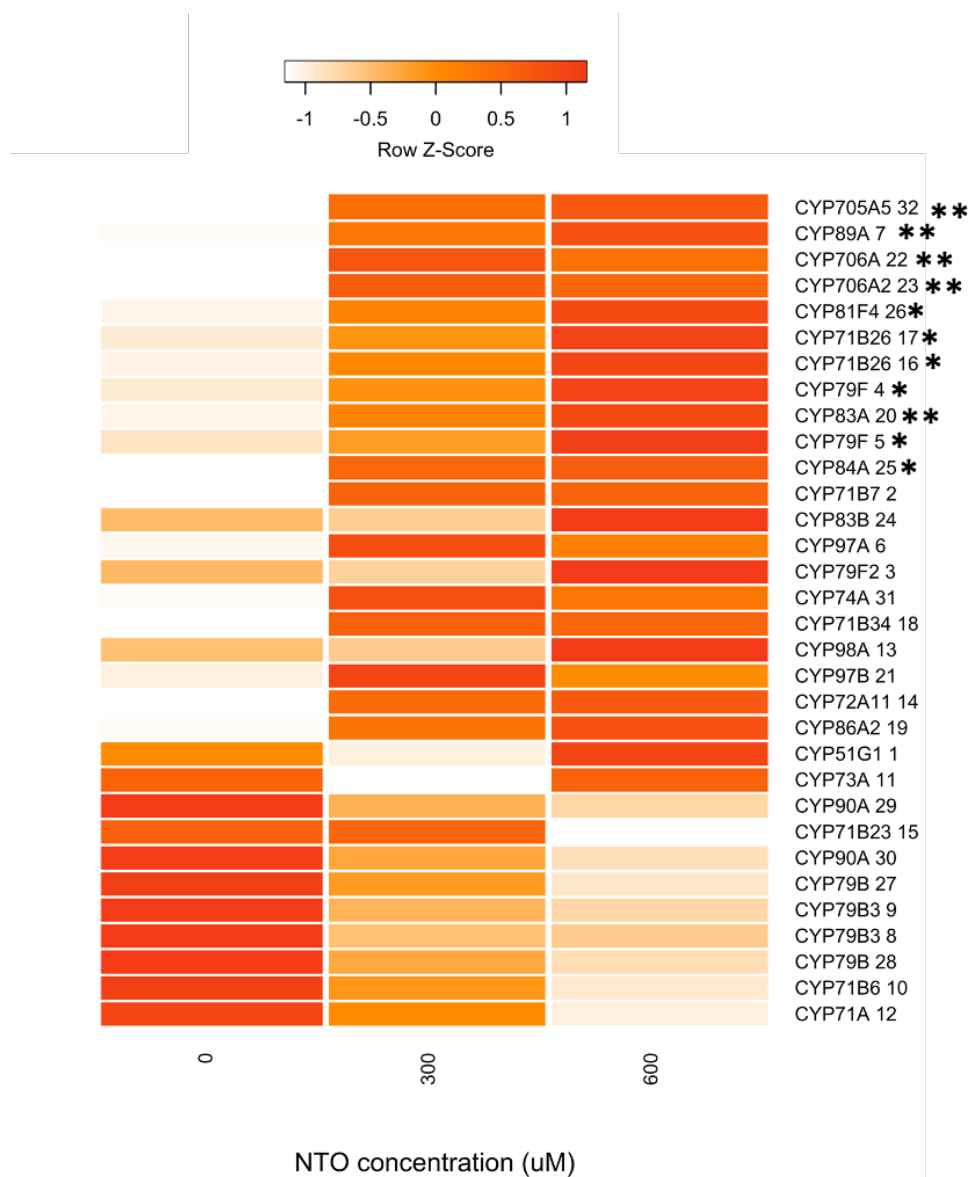


Figure 32. Abundance of Cytochrome P450 (CYP) Transcripts in Arabidopsis Plants Across a Range of NTO Concentrations.

** represents genes upregulated from undosed controls $P < 0.05$.*

Glutathione S-Transferases (GSTs) are a family of enzymes that catalyse conjugation of glutathione to electrophilic molecules and are associated with detoxification of xenobiotic compounds in plants (Gunning et al., 2014). Conjugation of glutathione to a xenobiotic occurs via the thiol group (Cummins et al., 2011). During NTO treatment, multiple GSTs exhibited large changes in expression levels and therefore may be linked to NTO detoxification. Three were selected for further analysis: AtGSTU5, AtGSTU16 and AtGSTU24. Codon-optimised sequences with an N-terminal His-tag in pET100 expression vectors (ThermoFischer Scientific) were obtained. The three recombinant GSTs were expressed in *E. coli*, purified and confirmed by Western Blot (Figure 33).

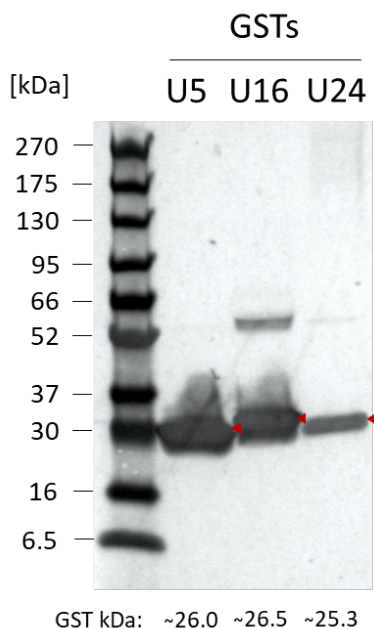


Figure 33. Western Blot of the Recombinantly Produced *A. thaliana* GSTs.

The relevant bands are indicated by the red markers. Theoretical molecular weights at the bottom of the blot were calculated using ExPASy ProtParam (Gasteiger et al., 2005).

GSTs can catalyse the conjugation of glutathione to a synthetic substrate 1-chloro-2,4-dinitrobenzene (CDNB) to form a dinitrophenyl thioether (GS-DNB) (Dixon et al., 2009; Gunning et al., 2014). To confirm the recombinant GSTs were active, each enzyme was incubated with glutathione and CDNB. The data indicated that both AtGSTU5 and AtGSTU24 were active.

Table 4. Specific activities of the GSTs in the presence of glutathione and CDNB substrates. Specific activity units are nmol substrate per minute per mg of enzyme. N.D. – No data.

AtGST	Specific activity (nmol min ⁻¹ mg ⁻¹)
AtGSTU5	2.1
AtGSTU16	N.D.
AtGSTU24	1.4

Next we sought to identify if the GSTs can catalyse conjugation of NTO to glutathione. Assays were set up *in vitro*, quenched and reaction products analysed by HPLC (Figure 34). No glutathione conjugates were detected on the HPLC traces. These data suggest that NTO is not a direct target for conjugation to glutathione by the GSTs.

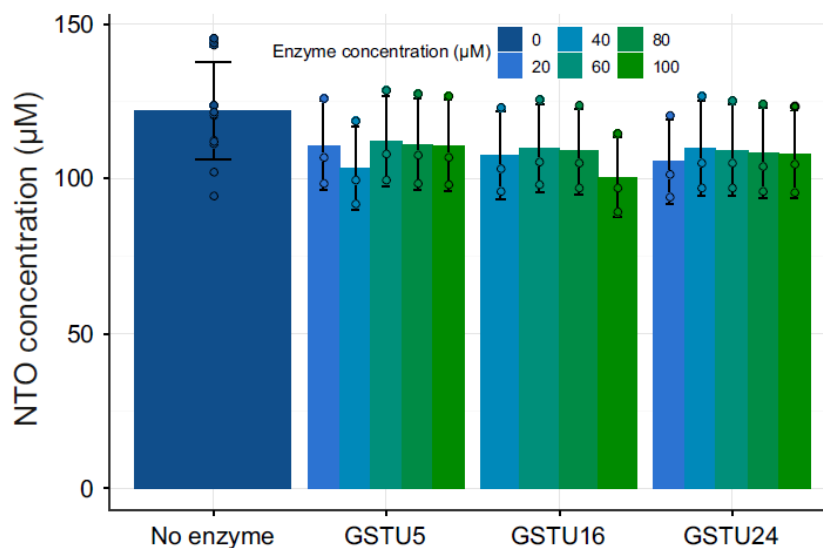


Figure 34. Concentrations of NTO Remaining after Incubating with GST Enzymes and Glutathione.

Data points are indicated for each bar (No enzyme was $n = 9 \pm SD$; all other samples $n = 3 \pm SD$). All data was not significantly different to the no enzyme control, calculated by one-way ANOVA and Tukey post-hoc test.

3.3.2 Task 6.2 Plant lines with modified target gene expression levels

3.3.2.1 T-DNA insertion plant lines

The transcriptomic data indicated that a number of genes were upregulated in the presence of 300 and 600 µM NTO. Mutant screening of plants in the presence of NTO were next carried out to establish if the genes have any role in NTO toxicity. Seed was obtained from NASC that contained Salk or Gabi-Kat T-DNA insertions within selected differentially-expressed genes. Homozygous lines were established for single or multiple alleles including the MATE efflux transporters *ALMT1* and *DTX18*, *Allene oxide cyclase 2 (AOC2)* and *SPX1*. In addition, *BBE/FOX1* lines were also obtained (downregulated in the transcriptomic analysis). Seeds were germinated and grown for 7 days on ½ MS agar with 0, 300 or 600 µM NTO, and then root lengths measured (Figure 35). Seedling biomass was visibly smaller (data not shown) and root lengths significantly reduced at 600 µM NTO. However, there was no significant difference between wildtype and mutant plant lines. The exception was *Almt1*^{-/-} under 0 µM NTO conditions which had shorter root lengths, possibly indicating a growth deficient phenotype.

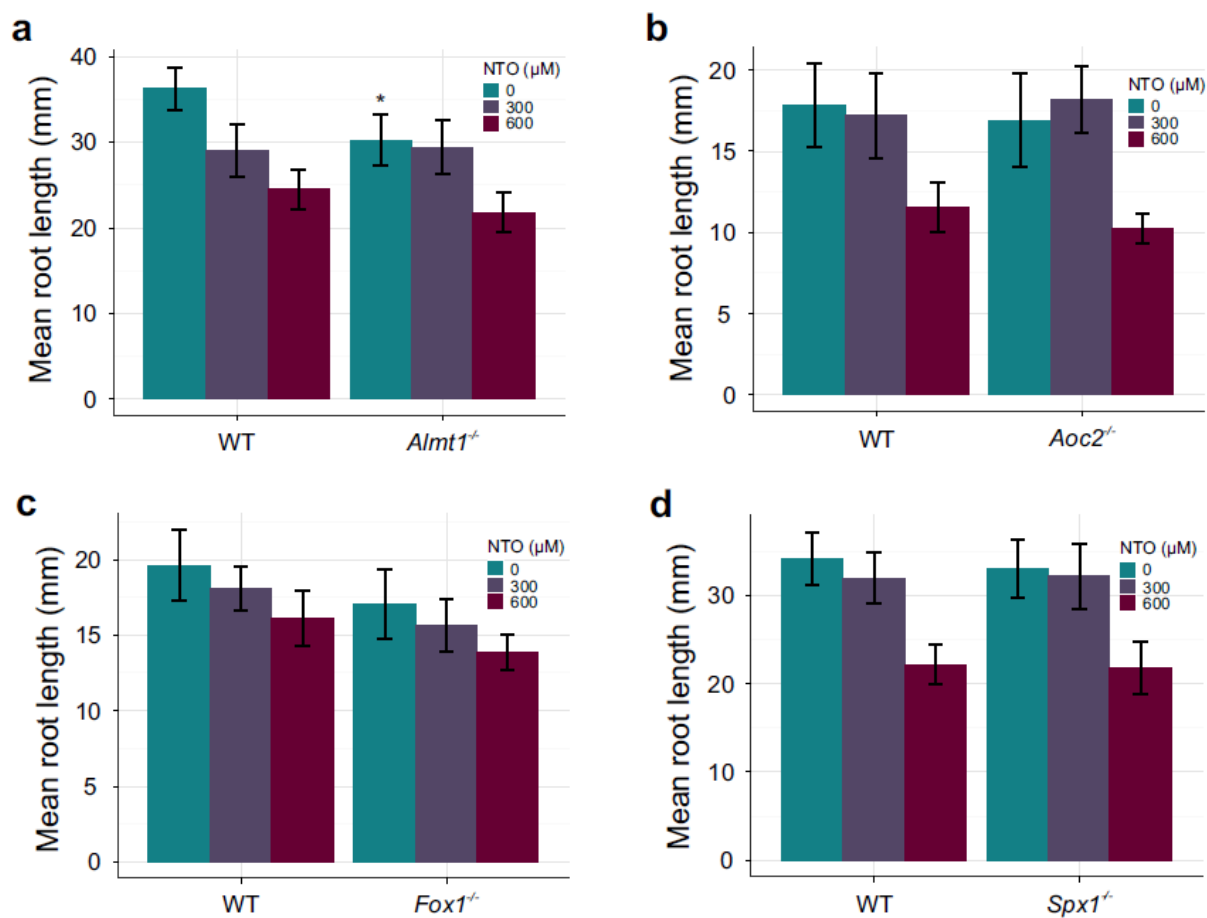


Figure 35. Root Lengths of Arabidopsis Plant Lines Grown on Different Concentrations of NTO.

Wildtype plants were grown alongside mutants of (a) *Almt1*, (b) *Aoc2*, (c) *Fox1* and (d) *Spx1*. All were grown under either 0, 300 or 600 μM NTO. Asterisks indicate statistical significance of mutant lines compared to wildtype plants under the same conditions. * $p < 0.05$. $n > 24 \pm SD$.

Though *Fox1* appears to be downregulated in the presence of NTO, previous transcriptomic analyses indicated that it is significantly upregulated in the presence of DNAN and TNT. To assess if *Fox1* has a role in the toxicity of DNAN and TNT, *Fox1* mutant lines were grown on agar plates containing either no compound, 50 μM DNAN or 7 μM TNT (Figure 36). However, no significant difference was observed to wildtype plants. The lack of any observable phenotypic differences in the mutant lines tested here is likely due to redundancy in xenobiotic detoxification pathways in plants.

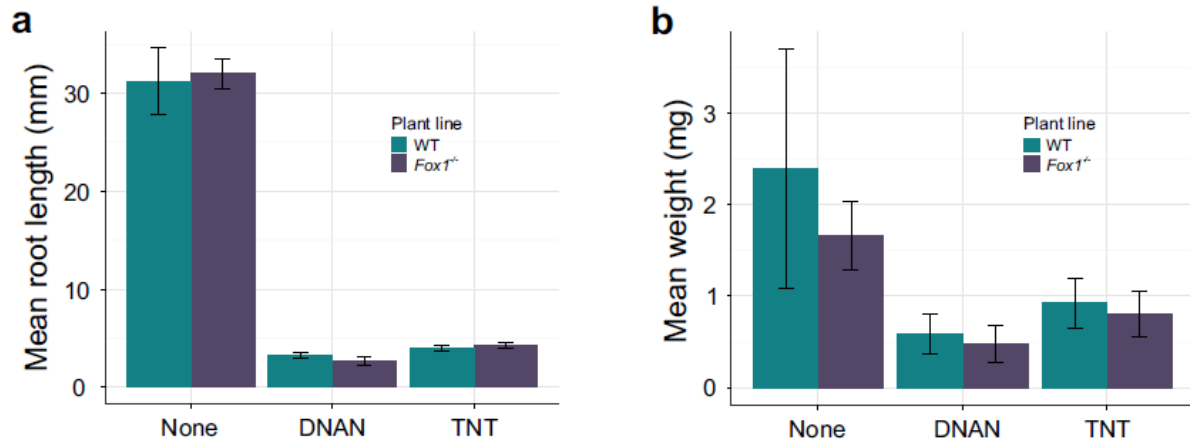


Figure 36. Growth of Wildtype and *Fox1* Mutant Lines Grown in the Presence DNAN and TNT.

Plant (a) root length was measured and (b) biomass weighed seven days after germination on $\frac{1}{2}$ MS agar plates. Error bars indicate standard deviation of replicates ($n \geq 27 \pm SD$).

4.0 CONCLUSIONS AND IMPLICATIONS FOR FUTURE RESEARCH/IMPLEMENTATION

The US EPA has classified TNT and RDX as possible carcinogens to humans, toxic to all organisms tested and recalcitrant to degradation in the soil (Rylott and Bruce, 2019). Pollution by these compounds remains a persistent issue. For example, explosives and chemical munitions from WW1 continue to contaminate the land around Verdun, France and pose a threat to human health (Gorecki et al., 2017). The US DoD previously estimated that to clean-up military training ranges alone would cost \$16-165 billion (U. S. Government Accountability, 2004). More recently, TNT and RDX have been replaced by less-shock sensitive DNAN and NTO compounds. The fate and impact of these new compounds on the environment is less well known, thus there is an urgent need to understand this in order to avoid greater environmental pollution and risks to human health. This project begins to determine the uptake and toxic effects of these insensitive munition compounds on plants.

4.1 OBJECTIVE 3. ELUCIDATED MECHANISMS OF DNAN AND NTO TOXICITY IN PLANTS

Little is known with regard to the mechanisms of DNAN and NTO toxicity in plants (Rylott et al., 2011b). However, uptake and toxicity of TNT has been previously characterised (Rylott et al., 2011a; Rylott and Bruce, 2009). Phytotoxicity of TNT is driven by the co-localized mitochondrial and plastidial form of MDHAR6 (Johnston et al., 2015). Given the structural similarity of DNAN, we hypothesized that MDHAR6 could also be involved in phytotoxicity of DNAN. Our data supports this hypothesis with MDHAR6-knockout plants demonstrating increased fitness to grow in DNAN-contaminated media (Figure 7) and soils (Figure 8). Moreover, recombinantly produced MDHAR6 had activity on DNAN, albeit much less than on TNT (Figure 9). MDHAR6-mediated toxicity of TNT is driven by a futile cycle of TNT itself. Reduction of TNT generates a nitro radical which then spontaneously regenerates to produce TNT and a superoxide radical. In addition, NADH is depleted during the reduction of TNT (Johnston et al., 2015). Our data also suggests this to be the same mechanism of plant toxicity to DNAN, given that MDHAR6 is active on DNAN but does not deplete the compound (Figure 9). Thus, inactivation of MDHAR6 could also enhance tolerance of plants to DNAN.

Mechanisms of NTO toxicity to plants is unknown, however NTO bears some chemical similarities with RDX (Toghiani et al., 2008). Plants can rapidly uptake RDX, however they have little inherent ability to degrade the compound (Cary et al., 2021; Just and Schnoor, 2004). Our data showed that seedling rootlengths were significantly reduced in 600 μ M NTO (Figure 4), but biomass of plants in shake flasks were unaffected up to 1000 μ M NTO (Figure 13). This is likely due to the different plant development stages used in each experiment (shake flask plants were germinated on media that did not contain NTO). Whereas TNT predominantly remains in the root, RDX is mostly translocated to aerial tissue. As a result, RDX breakdown in plants has been suggested to occur by photolysis (Just and Schnoor, 2004; Rylott et al., 2015; Vila et al., 2007). NTO has been shown to undergo photolysis in surface waters (Schroer et al., 2023). Therefore, it remains possible that the biomass of Arabidopsis plant is unaffected by NTO in our experiments due to the translocation of NTO into aerial tissue and undergoing photolysis. Further experiments are required to investigate this possibility.

4.2 OBJECTIVE 4. IDENTIFICATION OF THE *IN PLANTA* DETOXIFICATION INTERMEDIATES OF DNAN AND NTO IN ARABIDOPSIS

Metabolism of TNT generally occurs in the roots of plants in a series of reduction steps to generate HADNT and ADNT (Johnston et al., 2015; Rylott and Bruce, 2019). Prior to this project, little was known of the intermediates generated during metabolism of DNAN. However, one study that fed Arabidopsis plants with radio-labelled DNAN showed that DNAN was taken up and metabolised. Reduction products 2ANAN and 4ANAN were identified in plant tissue (Schroer et al., 2017). Our data confirms that plants can uptake and metabolise the compound. Interestingly, DNAN uptake was far slower than equivalent concentrations of TNT, indicative of slower breakdown of DNAN and a more chronic toxicity to the plant (Figure 10). We also identified the presence of 2ANAN and 4ANAN reduction products in plant tissue (Figure 11). Interestingly, DNAN and 2ANAN were identified in both the roots and shoots of plants (Figure 14). The presence of DNAN in aerial plant tissue also raises the prospect of a role of photolysis in breakdown of DNAN, as previously suggested (Rylott and Bruce, 2019; Schroer et al., 2017).

4.3 OBJECTIVE 5. RESOLVED BIOCHEMICAL PATHWAYS FOR THE DETOXIFICATION OF DNAN AND NTO IN PLANTS

In the presence of TNT, Arabidopsis plants upregulated a number of genes, including UGTs (Gandia-Herrero et al., 2008), GSTs (Gunning et al., 2014) and OPRs (Beynon et al., 2009). Transcriptomic analysis of RNA harvested from plants exposed to DNAN indicate significant differential expression of genes (Figure 16) with many associated with nitroreduction, conjugation and transport (Figure 17). Similar to TNT transcriptomic data, UGTs, GSTs and OPRs were all upregulated. Nine upregulated GSTs were recombinantly produced. However, assays with the recombinant GSTs indicated little to no conjugating activity of DNAN to GSH (Figure 20). UGTs were able to conjugate TNT reduction products HADNTs and, to a lesser extent, ADNTs to monoglucosides (Gandia-Herrero et al., 2008). Our transcriptomic analysis indicated upregulation of 21 UGTs which could also be involved in conjugation of DNAN (Figure 21). This warrants further investigation.

We also previously showed that OPRs form another part of the plants detoxification of TNT. The enzymes were able to generate nitro-reduced derivatives of TNT (Beynon et al., 2009). Our data indicated that OPR1, 2 and 4/5 were upregulated in the presence of DNAN (Figure 23). OPR4/5 enzymes were not thought to have any role in TNT detoxification *in planta* due to its relatively low expression in roots and reduced activity from a C-terminal truncation (Beynon et al., 2009). However, our analysis of DNAN and intermediates indicated high concentrations of both in roots and shoots. As OPR1 and 2 are predominantly expressed in plant roots (Beynon et al., 2009; Biesgen and Weiler, 1999), this suggested that OPR4/5 may have a role in detoxification of DNAN in plant aerial tissue. Recombinantly produced OPR1, 2 and 4/5 had demonstrable activity on DNAN (Figure 24) and overexpression plant lines indicated that OPR1-overexpressors could take up more DNAN from the media and OPR2-overexpressors generated more of the 2ANAN reduction product (Figure 25). Thus, though less active on DNAN compared to TNT, OPRs likely have a role in detoxification of DNAN in plants.

Our analysis also indicated that MRP2, a transporter associated with transporting xenobiotics (Hoffmann and Kroemer, 2004) was upregulated in response to DNAN. Moreover, the MRP family has also been shown to transport GSH and glutathione-conjugates in plants (Liu et al.,

2001). We generated knockout plant lines to identify if MRP2 has a role in breakdown of DNAN. However, no difference was observed to wildtype root lengths in the presence of DNAN. This could be due to redundancy in the transporters used to transport these molecules.

To date, no studies have been carried out on potential NTO detoxification pathways (Rylott and Bruce, 2019). Our transcriptomic analysis is the first to try and elucidate these pathways. Fewer genes were differentially expressed, compared to DNAN, indicative of NTO being much less toxic to plants (Figure 29). Nevertheless, a number of genes are upregulated including plant defensins (Figure 30), glycosyltransferases (Figure 31) and cytochrome P450s (Figure 32). Interestingly, plant defensins, of which have been associated with heavy metal tolerance (Mirouze et al., 2006), are not upregulated in response to DNAN. The reason for this is not known.

Cytochrome P450s are one of the most upregulated families in response to NTO. Indeed, this family of enzymes was also upregulated in response to TNT, RDX (Ekman et al., 2005) and DNAN in our analysis. The cytochrome P450 AT5G20150.1 was upregulated in response to RDX (Ekman et al., 2005) and NTO. The protein contains an SPX domain that has been associated with nutrient signalling (Duan et al., 2008; Secco et al., 2012; Wang et al., 2008). Finally, GSTs were also upregulated in response to NTO. Thus, three were recombinantly expressed and purified. However, no conjugation activity was observed for any of the enzymes on NTO to GSH (Figure 34).

Other individual genes MATE efflux transporter ALMT, AOC2 and SPX1 were upregulated in the NTO transcriptomic analysis. MATE efflux transporters are associated with metabolism of toxic compounds and organic acids (Qiao et al., 2020). AOC2 is a key enzyme involved in the production of jasmonic acid (Yang et al., 2023). Therefore, we decided to generate knockout plant lines of each in order to determine their contribution to detoxification of NTO. Though downregulated, FOX1 was included as it was upregulated in response to DNAN and TNT. Interestingly, FOX1 was upregulated alongside plant defensins in response to jasmonic acid treatment in Arabidopsis plants, a crucial signal molecule for plant defense against wounding (Pré et al., 2008). Moreover, AOC2 that is involved in biosynthesis of jasmonic acid was also upregulated in response to NTO. However, there was no difference in root lengths of seedlings compared to wild type (Figure 35 & Figure 36). This suggests that there is redundancy of the genes in the knockout plant lines.

4.4 CONCLUSION

DNAN appears to exert a more chronic toxicity on plants, with slower rates of uptake and metabolism. Like TNT, DNAN-mediated phytotoxicity was driven by MDHAR6. Plants were able to reduce DNAN to less toxic 2ANAN and 4ANAN intermediates throughout root and aerial tissue. As for TNT, numerous genes were upregulated in the presence of DNAN, including GSTs and OPRs. These contribute to breakdown of DNAN but proceed at much slower rates than for TNT. This may explain the more chronic toxicity observed. However, understanding these pathways will help in utilizing plants in phytoremediation of DNAN.

Our data showed that NTO was far less toxic to plants and toxicity effects were dependent on the developmental stage of the plant. Far fewer genes were differentially expressed in the presence of NTO and GSTs appeared to have little activity. Plant defense responses appeared most upregulated which could be due to pH-induced stress. These plants could serve as good foundation to express enzymes that can breakdown NTO and serve as a phytoremediation strategy.

5.0 LITERATURE CITED

- Ashburner, M., Ball, C.A., Blake, J.A., Botstein, D., Butler, H., Cherry, J.M., Davis, A.P., Dolinski, K., Dwight, S.S., Eppig, J.T., Harris, M.A., Hill, D.P., Issel-Tarver, L., Kasarskis, A., Lewis, S., Matese, J.C., Richardson, J.E., Ringwald, M., Rubin, G.M., Sherlock, G., 2000. Gene Ontology: tool for the unification of biology. *Nat. Genet.* 25, 25–29. <https://doi.org/10.1038/75556>
- Berardini, T.Z., Reiser, L., Li, D., Mezheritsky, Y., Muller, R., Strait, E., Huala, E., 2015. The arabidopsis information resource: Making and mining the “gold standard” annotated reference plant genome. *genesis* 53, 474–485. <https://doi.org/10.1002/dvg.22877>
- Beynon, E.R., Symons, Z.C., Jackson, R.G., Lorenz, A., Rylott, E.L., Bruce, N.C., 2009. The Role of Oxophytodienoate Reductases in the Detoxification of the Explosive 2,4,6-Trinitrotoluene by Arabidopsis. *Plant Physiol.* 151, 253–261. <https://doi.org/10.1104/pp.109.141598>
- Biesgen, C., Weiler, E.W., 1999. Structure and regulation of OPR1 and OPR2, two closely related genes encoding 12-oxophytodienoic acid-10,11-reductases from Arabidopsis thaliana. *Planta* 208, 155–165. <https://doi.org/10.1007/s004250050545>
- Breithaupt, C., Strassner, J., Breiting, U., Huber, R., Macheroux, P., Schaller, A., Clausen, T., 2001. X-Ray Structure of 12-Oxophytodienoate Reductase 1 Provides Structural Insight into Substrate Binding and Specificity within the Family of OYE. *Structure* 9, 419–429. [https://doi.org/10.1016/S0969-2126\(01\)00602-5](https://doi.org/10.1016/S0969-2126(01)00602-5)
- Cary, T.J., Rylott, E.L., Zhang, L., Routsong, R.M., Palazzo, A.J., Strand, S.E., Bruce, N.C., 2021. Field trial demonstrating phytoremediation of the military explosive RDX by XplA/XplB-expressing switchgrass. *Nat. Biotechnol.* 39, 1216–1219. <https://doi.org/10.1038/s41587-021-00909-4>
- Coleman, J., Blake-Kalff, M., Davies, E., 1997. Detoxification of xenobiotics by plants: chemical modification and vacuolar compartmentation. *Trends Plant Sci.* 2, 144–151. [https://doi.org/10.1016/S1360-1385\(97\)01019-4](https://doi.org/10.1016/S1360-1385(97)01019-4)
- Cummins, I., Dixon, D.P., Freitag-Pohl, S., Skipsey, M., Edwards, R., 2011. Multiple roles for plant glutathione transferases in xenobiotic detoxification. *Drug Metab. Rev.* 43, 266–280. <https://doi.org/10.3109/03602532.2011.552910>
- Dixon, D.P., Hawkins, T., Hussey, P.J., Edwards, R., 2009. Enzyme activities and subcellular localization of members of the Arabidopsis glutathione transferase superfamily. *J. Exp. Bot.* 60, 1207–1218. <https://doi.org/10.1093/jxb/ern365>
- Dodard, S.G., Sarrazin, M., Hawari, J., Paquet, L., Ampleman, G., Thiboutot, S., Sunahara, G.I., 2013. Ecotoxicological assessment of a high energetic and insensitive munitions compound: 2,4-Dinitroanisole (DNAN). *J. Hazard. Mater.* 262, 143–150. <https://doi.org/10.1016/j.jhazmat.2013.08.043>
- Duan, K., Yi, K., Dang, L., Huang, H., Wu, W., Wu, P., 2008. Characterization of a sub-family of Arabidopsis genes with the SPX domain reveals their diverse functions in plant tolerance to phosphorus starvation. *Plant J.* 54, 965–975. <https://doi.org/10.1111/j.1365-313X.2008.03460.x>

- Ekman, D.R., Wolfe, N.L., Dean, J.F.D., 2005. Gene Expression Changes in *Arabidopsis thaliana* Seedling Roots Exposed to the Munition Hexahydro-1,3,5-trinitro-1,3,5-triazine. *Environ. Sci. Technol.* 39, 6313–6320. <https://doi.org/10.1021/es050385r>
- Fida, T.T., Palamuru, S., Pandey, G., Spain, J.C., 2014. Aerobic Biodegradation of 2,4-Dinitroanisole by *Nocardioide* sp. Strain JS1661. *Appl. Environ. Microbiol.* 80, 7725–7731. <https://doi.org/10.1128/AEM.02752-14>
- Gandia-Herrero, F., Lorenz, A., Larson, T., Graham, I.A., Bowles, D.J., Rylott, E.L., Bruce, N.C., 2008. Detoxification of the explosive 2,4,6-trinitrotoluene in *Arabidopsis*: discovery of bifunctional O- and C-glucosyltransferases. *Plant J.* 56, 963–974. <https://doi.org/10.1111/j.1365-3113X.2008.03653.x>
- Gasteiger, E., Hoogland, C., Gattiker, A., Duvaud, S., Wilkins, M.R., Appel, R.D., Bairoch, A., 2005. Protein Identification and Analysis Tools on the ExPASy Server, in: Walker, J.M. (Ed.), *The Proteomics Protocols Handbook*, Springer Protocols Handbooks. Humana Press, Totowa, NJ, pp. 571–607. <https://doi.org/10.1385/1-59259-890-0:571>
- Gorecki, S., Nesslany, F., Hubé, D., Mullot, J.-U., Vasseur, P., Marchioni, E., Camel, V., Noël, L., Le Bizec, B., Guérin, T., Feidt, C., Archer, X., Mahe, A., Rivière, G., 2017. Human health risks related to the consumption of foodstuffs of plant and animal origin produced on a site polluted by chemical munitions of the First World War. *Sci. Total Environ.* 599–600, 314–323. <https://doi.org/10.1016/j.scitotenv.2017.04.213>
- Gunning, V., Tzafestas, K., Sparrow, H., Johnston, E.J., Brentnall, A.S., Potts, J.R., Rylott, E.L., Bruce, N.C., 2014. *Arabidopsis* Glutathione Transferases U24 and U25 Exhibit a Range of Detoxification Activities with the Environmental Pollutant and Explosive, 2,4,6-Trinitrotoluene. *Plant Physiol.* 165, 854–865. <https://doi.org/10.1104/pp.114.237180>
- Haley, M.V., Kuperman, R.G., Checkai, R.T., 2009. Aquatic Toxicity of 3-Nitro-1,2,4-Triazol-5-One. Edgewood Chemical Biological Center.
- Hawari, J., Monteil-Rivera, F., Perreault, N.N., Halasz, A., Paquet, L., Radovic-Hrapovic, Z., Deschamps, S., Thiboutot, S., Ampleman, G., 2015. Environmental fate of 2,4-dinitroanisole (DNAN) and its reduced products. *Chemosphere* 119, 16–23. <https://doi.org/10.1016/j.chemosphere.2014.05.047>
- Hoffmann, U., Kroemer, H.K., 2004. The ABC Transporters MDR1 and MRP2: Multiple Functions in Disposition of Xenobiotics and Drug Resistance. *Drug Metab. Rev.* 36, 669–701. <https://doi.org/10.1081/DMR-200033473>
- Johnston, E.J., Rylott, E.L., Beynon, E., Lorenz, A., Chechik, V., Bruce, N.C., 2015. Monodehydroascorbate reductase mediates TNT toxicity in plants. *Science* 349, 1072–1075. <https://doi.org/10.1126/science.aab3472>
- Just, C.L., Schnoor, J.L., 2004. Photophotolysis of Hexahydro-1,3,5-trinitro-1,3,5-triazine (RDX) in Leaves of Reed Canary Grass. *Environ. Sci. Technol.* 38, 290–295. <https://doi.org/10.1021/es034744z>
- Kang, J., Yim, S., Choi, H., Kim, A., Lee, K.P., Lopez-Molina, L., Martinoia, E., Lee, Y., 2015. Absciscic acid transporters cooperate to control seed germination. *Nat. Commun.* 6, 8113. <https://doi.org/10.1038/ncomms9113>

- Karthikeyan, S., Spain, J.C., 2016. Biodegradation of 2,4-dinitroanisole (DNAN) by *Nocardioides* sp. JS1661 in water, soil and bioreactors. *J. Hazard. Mater.* 312, 37–44. <https://doi.org/10.1016/j.jhazmat.2016.03.029>
- Klein, M., Burla, B., Martinoia, E., 2006. The multidrug resistance-associated protein (MRP/ABCC) subfamily of ATP-binding cassette transporters in plants. *FEBS Lett.* 580, 1112–1122. <https://doi.org/10.1016/j.febslet.2005.11.056>
- Kumar, S., Trivedi, P.K., 2018. Glutathione S-Transferases: Role in Combating Abiotic Stresses Including Arsenic Detoxification in Plants. *Front. Plant Sci.* 9.
- Lamesch, P., Berardini, T.Z., Li, D., Swarbreck, D., Wilks, C., Sasidharan, R., Muller, R., Dreher, K., Alexander, D.L., Garcia-Hernandez, M., Karthikeyan, A.S., Lee, C.H., Nelson, W.D., Ploetz, L., Singh, S., Wensel, A., Huala, E., 2012. The Arabidopsis Information Resource (TAIR): improved gene annotation and new tools. *Nucleic Acids Res.* 40, D1202–D1210. <https://doi.org/10.1093/nar/gkr1090>
- Landa, P., Storchova, H., Hodek, J., Vankova, R., Podlipna, R., Marsik, P., Ovesna, J., Vanek, T., 2010. Transferases and transporters mediate the detoxification and capacity to tolerate trinitrotoluene in Arabidopsis. *Funct. Integr. Genomics* 10, 547–559. <https://doi.org/10.1007/s10142-010-0176-1>
- Le Campion, L., Vandais, A., Ouazzani, J., 1999. Microbial remediation of NTO in aqueous industrial wastes. *FEMS Microbiol. Lett.* 176, 197–203. <https://doi.org/10.1111/j.1574-6968.1999.tb13662.x>
- Lee, M., Lee, K., Lee, J., Noh, E.W., Lee, Y., 2005. AtPDR12 Contributes to Lead Resistance in Arabidopsis. *Plant Physiol.* 138, 827–836. <https://doi.org/10.1104/pp.104.058107>
- Lent, E.M., Narizzano, A.M., Koistinen, K.A., Johnson, M.S., 2020. Chronic oral toxicity of 3-nitro-1,2,4-triazol-5-one (NTO) in rats. *Regul. Toxicol. Pharmacol.* 112, 104609. <https://doi.org/10.1016/j.yrtph.2020.104609>
- Liang, J., Olivares, C., Field, J.A., Sierra-Alvarez, R., 2013. Microbial toxicity of the insensitive munitions compound, 2,4-dinitroanisole (DNAN), and its aromatic amine metabolites. *J. Hazard. Mater.* 262, 281–287. <https://doi.org/10.1016/j.jhazmat.2013.08.046>
- Lisenbee, C.S., Lingard, M.J., Trelease, R.N., 2005. Arabidopsis peroxisomes possess functionally redundant membrane and matrix isoforms of monodehydroascorbate reductase. *Plant J.* 43, 900–914. <https://doi.org/10.1111/j.1365-313X.2005.02503.x>
- Liu, C.-J., Miao, Y.-C., Zhang, K.-W., 2011. Sequestration and Transport of Lignin Monomeric Precursors. *Molecules* 16, 710–727. <https://doi.org/10.3390/molecules16010710>
- Liu, G., Sánchez-Fernández, R., Li, Z.-S., Rea, P.A., 2001. Enhanced Multispecificity of Arabidopsis Vacuolar Multidrug Resistance-associated Protein-type ATP-binding Cassette Transporter, AtMRP2*. *J. Biol. Chem.* 276, 8648–8656. <https://doi.org/10.1074/jbc.M009690200>
- Lu, Y.-P., Li, Z.-S., Rea, P.A., 1997. AtMRP1 gene of Arabidopsis encodes a glutathione S-conjugate pump: Isolation and functional definition of a plant ATP-binding cassette transporter gene. *Proc. Natl. Acad. Sci. U. S. A.* 94, 8243–8248.

- Madeira, C.L., Field, J.A., Simonich, M.T., Tanguay, R.L., Chorover, J., Sierra-Alvarez, R., 2018. Ecotoxicity of the insensitive munitions compound 3-nitro-1,2,4-triazol-5-one (NTO) and its reduced metabolite 3-amino-1,2,4-triazol-5-one (ATO). *J. Hazard. Mater.* 343, 340–346. <https://doi.org/10.1016/j.jhazmat.2017.09.052>
- Mirouze, M., Sels, J., Richard, O., Czernic, P., Loubet, S., Jacquier, A., François, I.E.J.A., Cammue, B.P.A., Lebrun, M., Berthomieu, P., Marquès, L., 2006. A putative novel role for plant defensins: a defensin from the zinc hyper-accumulating plant, *Arabidopsis halleri*, confers zinc tolerance. *Plant J.* 47, 329–342. <https://doi.org/10.1111/j.1365-313X.2006.02788.x>
- Murashige, T., Skoog, F., 1962. A Revised Medium for Rapid Growth and Bio Assays with Tobacco Tissue Cultures. *Physiol. Plant.* 15, 473–497. <https://doi.org/10.1111/j.1399-3054.1962.tb08052.x>
- Ohkama-Ohtsu, N., Zhao, P., Xiang, C., Oliver, D.J., 2007. Glutathione conjugates in the vacuole are degraded by γ -glutamyl transpeptidase GGT3 in *Arabidopsis*. *Plant J.* 49, 878–888. <https://doi.org/10.1111/j.1365-313X.2006.03005.x>
- Olivares, C., Liang, J., Abrell, L., Sierra-Alvarez, R., Field, J.A., 2013. Pathways of reductive 2,4-dinitroanisole (DNAN) biotransformation in sludge. *Biotechnol. Bioeng.* 110, 1595–1604. <https://doi.org/10.1002/bit.24820>
- Olivares, C.I., Abrell, L., Khatiwada, R., Chorover, J., Sierra-Alvarez, R., Field, J.A., 2016a. (Bio)transformation of 2,4-dinitroanisole (DNAN) in soils. *J. Hazard. Mater.* 304, 214–221. <https://doi.org/10.1016/j.jhazmat.2015.10.059>
- Olivares, C.I., Sierra-Alvarez, R., Abrell, L., Chorover, J., Simonich, M., Tanguay, R.L., Field, J.A., 2016b. Zebrafish embryo toxicity of anaerobic biotransformation products from the insensitive munitions compound 2,4-dinitroanisole. *Environ. Toxicol. Chem.* 35, 2774–2781. <https://doi.org/10.1002/etc.3446>
- Perreault, N.N., Manno, D., Halasz, A., Thiboutot, S., Ampleman, G., Hawari, J., 2012. Aerobic biotransformation of 2,4-dinitroanisole in soil and soil *Bacillus* sp. *Biodegradation* 23, 287–295. <https://doi.org/10.1007/s10532-011-9508-7>
- Platten, W.E., Bailey, D., Suidan, M.T., Maloney, S.W., 2010. Biological transformation pathways of 2,4-dinitro anisole and N-methyl paranitro aniline in anaerobic fluidized-bed bioreactors. *Chemosphere* 81, 1131–1136. <https://doi.org/10.1016/j.chemosphere.2010.08.044>
- Pré, M., Atallah, M., Champion, A., De Vos, M., Pieterse, C.M.J., Memelink, J., 2008. The AP2/ERF Domain Transcription Factor ORA59 Integrates Jasmonic Acid and Ethylene Signals in Plant Defense. *Plant Physiol.* 147, 1347–1357. <https://doi.org/10.1104/pp.108.117523>
- Qiao, C., Yang, J., Wan, Y., Xiang, S., Guan, M., Du, H., Tang, Z., Lu, K., Li, J., Qu, C., 2020. A Genome-Wide Survey of MATE Transporters in Brassicaceae and Unveiling Their Expression Profiles under Abiotic Stress in Rapeseed. *Plants* 9, 1072. <https://doi.org/10.3390/plants9091072>
- Ramel, F., Sulmon, C., Serra, A.-A., Gouesbet, G., Couée, I., 2012. Xenobiotic sensing and signalling in higher plants. *J. Exp. Bot.* 63, 3999–4014. <https://doi.org/10.1093/jxb/ers102>

- Richard, T., Weidhaas, J., 2014. Dissolution, sorption, and phytoremediation of IMX-101 explosive formulation constituents: 2,4-dinitroanisole (DNAN), 3-nitro-1,2,4-triazol-5-one (NTO), and nitroguanidine. *J. Hazard. Mater.* 280, 561–569. <https://doi.org/10.1016/j.jhazmat.2014.08.042>
- Robinson, M.D., McCarthy, D.J., Smyth, G.K., 2010. edgeR: a Bioconductor package for differential expression analysis of digital gene expression data. *Bioinformatics* 26, 139–140. <https://doi.org/10.1093/bioinformatics/btp616>
- Ross, J., Li, Y., Lim, E.-K., Bowles, D.J., 2001. Higher plant glycosyltransferases. *Genome Biol.* 2, reviews3004.1. <https://doi.org/10.1186/gb-2001-2-2-reviews3004>
- Rylott, E.L., Bruce, N.C., 2019. Right on target: using plants and microbes to remediate explosives. *Int. J. Phytoremediation* 21, 1051–1064. <https://doi.org/10.1080/15226514.2019.1606783>
- Rylott, E.L., Bruce, N.C., 2009. Plants disarm soil: engineering plants for the phytoremediation of explosives. *Trends Biotechnol.* 27, 73–81. <https://doi.org/10.1016/j.tibtech.2008.11.001>
- Rylott, E.L., Budarina, M.V., Barker, A., Lorenz, A., Strand, S.E., Bruce, N.C., 2011a. Engineering plants for the phytoremediation of RDX in the presence of the co-contaminating explosive TNT. *New Phytol.* 192, 405–413. <https://doi.org/10.1111/j.1469-8137.2011.03807.x>
- Rylott, E.L., Johnston, E.J., Bruce, N.C., 2015. Harnessing microbial gene pools to remediate persistent organic pollutants using genetically modified plants—a viable technology? *J. Exp. Bot.* 66, 6519–6533. <https://doi.org/10.1093/jxb/erv384>
- Rylott, E.L., Lorenz, A., Bruce, N.C., 2011b. Biodegradation and biotransformation of explosives. *Curr. Opin. Biotechnol., Energy biotechnology – Environmental biotechnology* 22, 434–440. <https://doi.org/10.1016/j.copbio.2010.10.014>
- Schroer, H.W., Langenfeld, K.L., Li, X., Lehmler, H.-J., Just, C.L., 2015. Stable Isotope-Enabled Pathway Elucidation of 2,4-Dinitroanisole Metabolized by *Rhizobium litchii*. *Environ. Sci. Technol. Lett.* 2, 362–366. <https://doi.org/10.1021/acs.estlett.5b00278>
- Schroer, H.W., Li, X., Lehmler, H.-J., Just, C.L., 2017. Metabolism and Photolysis of 2,4-Dinitroanisole in *Arabidopsis*. *Environ. Sci. Technol.* 51, 13714–13722. <https://doi.org/10.1021/acs.est.7b04220>
- Schroer, H.W., Londono, E., Li, X., Lehmler, H.-J., Arnold, W., Just, C.L., 2023. Photolysis of 3-Nitro-1,2,4-triazol-5-one: Mechanisms and Products. *ACS EST Water* 3, 783–792. <https://doi.org/10.1021/acsestwater.2c00567>
- Secco, D., Wang, C., Arpat, B.A., Wang, Z., Poirier, Y., Tyerman, S.D., Wu, P., Shou, H., Whelan, J., 2012. The emerging importance of the SPX domain-containing proteins in phosphate homeostasis. *New Phytol.* 193, 842–851. <https://doi.org/10.1111/j.1469-8137.2011.04002.x>
- Taguchi, G., Ubukata, T., Nozue, H., Kobayashi, Y., Takahi, M., Yamamoto, H., Hayashida, N., 2010. Malonylation is a key reaction in the metabolism of xenobiotic phenolic glucosides in *Arabidopsis* and tobacco. *Plant J.* 63, 1031–1041. <https://doi.org/10.1111/j.1365-313X.2010.04298.x>

- Taylor, S., Park, E., Bullion, K., Dontsova, K., 2015. Dissolution of three insensitive munitions formulations. *Chemosphere* 119, 342–348.
<https://doi.org/10.1016/j.chemosphere.2014.06.050>
- The Gene Ontology Consortium, 2019. The Gene Ontology Resource: 20 years and still GOing strong. *Nucleic Acids Res.* 47, D330–D338. <https://doi.org/10.1093/nar/gky1055>
- Toghiani, R.K., Toghiani, H., Maloney, S.W., Boddu, V.M., 2008. Prediction of physicochemical properties of energetic materials. *Fluid Phase Equilibria* 264, 86–92.
<https://doi.org/10.1016/j.fluid.2007.10.018>
- Tzafestas, K., Razalan, M.M., Gyulev, I., Mazari, A.M.A., Mannervik, B., Rylott, E.L., Bruce, N.C., 2017. Expression of a *Drosophila* glutathione transferase in *Arabidopsis* confers the ability to detoxify the environmental pollutant, and explosive, 2,4,6-trinitrotoluene. *New Phytol.* 214, 294–303. <https://doi.org/10.1111/nph.14326>
- U. S. Government Accountability, O., 2004. DOD Operational Ranges: More Reliable Cleanup Cost Estimates and a Proactive Approach to Identifying Contamination Are Needed | U.S. GAO [WWW Document]. URL <https://www.gao.gov/products/gao-04-601> (accessed 1.8.24).
- Vila, M., Lorber-Pascal, S., Laurent, F., 2007. Fate of RDX and TNT in agronomic plants. *Environ. Pollut.* 148, 148–154. <https://doi.org/10.1016/j.envpol.2006.10.030>
- Wang, Y., Secco, D., Poirier, Y., 2008. Characterization of the PHO1 Gene Family and the Responses to Phosphate Deficiency of *Physcomitrella patens*. *Plant Physiol.* 146, 323–324.
<https://doi.org/10.1104/pp.107.108548>
- Yang, L., Sun, Q., Geng, B., Shi, J., Zhu, H., Sun, Y., Yang, Q., Yang, B., Guo, Z., 2023. Jasmonate biosynthesis enzyme allene oxide cyclase 2 mediates cold tolerance and pathogen resistance. *Plant Physiol.* 193, 1621–1634.
<https://doi.org/10.1093/plphys/kiad362>